

# HETE-2 Localizations and Observations of Four Short Gamma-Ray Bursts: GRBs 010326B, 040802, 051211 and 060121

T. Q. Donaghy,<sup>1</sup> D. Q. Lamb,<sup>1</sup> T. Sakamoto,<sup>2</sup> J. P. Norris,<sup>2</sup> Y. Nakagawa,<sup>3</sup> J. Villasenor,<sup>4</sup>  
J.-L. Atteia,<sup>5</sup> R. Vanderspek,<sup>4</sup> C. Graziani,<sup>1</sup> N. Kawai,<sup>6,7</sup> G. R. Ricker,<sup>4</sup> G. B. Crew,<sup>4</sup>  
J. Doty,<sup>18,4</sup> G. Prigozhin,<sup>4</sup> J. G. Jernigan,<sup>8</sup> Y. Shirasaki,<sup>9,7</sup> M. Suzuki,<sup>6</sup> N. Butler,<sup>8,4</sup>  
K. Hurley,<sup>8</sup> T. Tamagawa,<sup>7</sup> A. Yoshida,<sup>3,7</sup> M. Matsuoka,<sup>11</sup> E. E. Fenimore,<sup>10</sup> M. Galassi,<sup>10</sup>  
M. Boer,<sup>12,21</sup> J.-P. Dezalay,<sup>12</sup> J.-F. Olive,<sup>12</sup> A. Levine,<sup>4</sup> F. Martel,<sup>19,4</sup> E. Morgan,<sup>4</sup> R. Sato,<sup>6</sup>  
S. E. Woosley,<sup>13</sup> J. Braga,<sup>14</sup> R. Manchanda,<sup>15</sup> G. Pizzichini,<sup>16</sup> K. Takagishi,<sup>17</sup>  
and M. Yamauchi<sup>17</sup>

## ABSTRACT

Here we report the localizations and properties of four short-duration GRBs localized by the High Energy Transient Explorer 2 satellite (HETE-2): GRBs

---

<sup>1</sup>Department of Astronomy and Astrophysics, University of Chicago, 5640 South Ellis Avenue, Chicago, IL 60637.

<sup>4</sup>MIT Kavli Institute, Massachusetts Institute of Technology, 70 Vassar Street, Cambridge, MA, 02139.

<sup>3</sup>Department of Physics, Aoyama Gakuin University, Chitosedai 6-16-1 Setagaya-ku, Tokyo 157-8572, Japan.

<sup>5</sup>Laboratoire d’Astrophysique, Observatoire Midi-Pyrénées, 14 Ave. E. Belin, 31400 Toulouse, France.

<sup>6</sup>Department of Physics, Tokyo Institute of Technology, 2-12-1 Ookayama, Meguro-ku, Tokyo 152-8551, Japan.

<sup>7</sup>RIKEN (Institute of Physical and Chemical Research), 2-1 Hirosawa, Wako, Saitama 351-0198, Japan.

<sup>8</sup>University of California at Berkeley, Space Sciences Laboratory, Berkeley, CA, 94720-7450.

<sup>9</sup>National Astronomical Observatory, Osawa 2-21-1, Mitaka, Tokyo 181-8588 Japan.

<sup>10</sup>Los Alamos National Laboratory, P.O. Box 1663, Los Alamos, NM, 87545.

<sup>11</sup>Tsukuba Space Center, National Space Development Agency of Japan, Tsukuba, Ibaraki, 305-8505, Japan.

<sup>12</sup>Centre d’Etude Spatiale des Rayonnements, Observatoire Midi-Pyrénées, 9 Ave. de Colonel Roche, 31028 Toulouse Cedex 4, France.

<sup>13</sup>Department of Astronomy and Astrophysics, University of California at Santa Cruz, 477 Clark Kerr Hall, Santa Cruz, CA 95064.

<sup>2</sup>NASA Goddard Space Flight Center, Greenbelt, MD, 20771.

<sup>14</sup>Instituto Nacional de Pesquisas Espaciais, Avenida Dos Astronautas 1758, São José dos Campos 12227-010, Brazil.

<sup>15</sup>Department of Astronomy and Astrophysics, Tata Institute of Fundamental Research, Homi Bhabha Road, Mumbai, 400 005, India.

<sup>16</sup>INAF/IASF Bologna, via Gobetti 101, 40129 Bologna, Italy.

<sup>17</sup>Faculty of engineering, Miyazaki University, Gakuen Kibanadai Nishi, Miyazaki 889-2192, Japan.

<sup>18</sup>Noqsi Aerospace, Ltd., 2822 South Nova Road, Pine, CO 80470.

<sup>19</sup>Espace Inc., 30 Lynn Avenue, Hull, MA 02045.

<sup>20</sup>Department of Earth and Space Science, Graduate School of Science, Osaka University, 1-1 Machikaneyama-cho, Toyonaka, Osaka, 560-0043, Japan.

<sup>21</sup>Observatoire de Haute Provence, 04870 St. Michel l’Observatoire, France.

010326B, 040802, 051211 and 060121, all of which were detected by the French Gamma Telescope (Fregate) and localized with the Wide-field X-ray Monitor (WXM) and/or Soft X-ray Camera (SXC) instruments. We discuss ten possible criteria for determining whether these GRBs are “short population bursts” (SPBs) or “long population bursts” (LPBs). These criteria are (1) duration, (2) pulse widths, (3) spectral hardness, (4) spectral lag, (5) energy  $E_\gamma$  radiated in gamma rays (or equivalently, the kinetic energy  $E_{\text{KE}}$  of the GRB jet), (6) existence of a long, soft bump following the burst, (7) location of the burst in the host galaxy, (8) lack of detection of a supernova component to deep limits, (9) type of host galaxy and (10) detection of gravitational waves. In particular, we have developed a likelihood method for determining the probability that a burst is an SPB or a LPB on the basis of its  $T_{90}$  duration alone. A striking feature of the resulting probability distribution is that the  $T_{90}$  duration at which a burst has an equal probability of being a SPB or a LPB is  $T_{90} = 5$  s, *not*  $T_{90} = 2$  s, which is the criterion that is often used to separate the two populations. The four short-duration bursts discussed in detail in this paper have  $T_{90}$  durations in the Fregate 30-400 keV energy band of 1.90, 2.31, 4.25, and 1.97 sec, respectively, yielding probabilities  $P(S|T_{90}) = 0.97, 0.91, 0.60,$  and  $0.95$  that these bursts are SPBs on the basis of their  $T_{90}$  durations alone. All four bursts also have spectral lags consistent with zero. These results provide strong evidence that all four GRBs are SPBs.

Focusing further on the remarkable properties of GRB 060121, we present the results of a detailed analysis of the light curve and time-resolved spectroscopy of GRB 060121. The former reveals the presence of a long, soft bump typical of those seen in the light curves of SPBs. This provides additional strong evidence that GRB 060121 is an SPB. The latter reveals the existence of dramatic spectral evolution during the burst, making this burst one of only a few SPBs for which strong spectral evolution has been demonstrated. We find that the spectral evolution exhibited by GRB 060121 obeys the Amati et al. (2002) relation internally.

GRB 060121 is also the first SPB for which it has been possible to obtain a photometric redshift from the optical and NIR afterglow of the burst. The result provides strong evidence that GRB 060121 lies at a redshift  $z > 1.5$ , and most likely at a redshift  $z = 4.6$ , making this the first short burst for which a high redshift has been securely determined. At either redshift, its  $E_{\text{iso}}$  and  $E_{\text{peak}}^{\text{obs}}$  values are consistent with the Amati et al. (2002) relation. However, adopting the jet opening angles derived from modeling of its afterglow the values of  $E_\gamma$  are  $3.0 \times 10^{49}$  ergs if  $z = 1.5$  and  $1.3 \times 10^{49}$  ergs if  $z = 4.6$ . These values are similar to

those of the SPBs GRB 050709 and GRB 050724 and  $\sim 100$  times smaller than those of almost all other hard GRBs. They therefore provide additional evidence that GRB 060121 is a SPB. HST observations have shown that the probable host galaxy of GRB 060121 is irregularly shaped and undergoing star formation. The location of GRB 060121 appears not to be coincident with the strongest star forming regions in the galaxy, which provides additional evidence that it is an SPB. Thus, all of the attributes of GRB 060121, when taken together, make a strong, although not conclusive case, that GRB 060121 is an SPB. If GRB 060121 is due to the merger of a compact binary, its high redshift and probable origin in a star-forming galaxy argue for a progenitor population for SPBs that is diverse in terms of merger times and locations.

*Subject headings:* gamma rays: bursts (GRB 010326B, GRB 040802, GRB 051211, GRB 060121) – binaries: close – stars: neutron – black hole physics

## 1. Introduction

Gamma-Ray Bursts (GRBs) are thought to belong to two populations: short bursts and long bursts (Mazets & Golenetskii 1981; Hurley 1992; Lamb, Graziani & Smith 1993; Kouveliotou et al. 1992). The localizations by HETE-2 (Ricker et al. 2003) and Swift of three “short population bursts” (SPBs) during the summer of 2005 have solved in large part the mystery of SPBs. The localization of GRB 050509B by Swift led to the first detection of the X-ray afterglow of a short GRB, which was found to lie in the vicinity of a large elliptical galaxy at redshift  $z = 0.225$  (Gehrels et al. 2005). The first detection of an afterglow for a SPB implied that such bursts also have detectable optical afterglows, and held out the promise that the precise localization of the optical afterglow of a short GRB would lead to the identification of the host and a secure measurement of the redshift of a short GRB.

It was not long before this promise was fulfilled. The localization of GRB 050709 by HETE-2 (Villasenor et al. 2005) led to several firsts for a SPB: (1) the first detection of an optical afterglow (Hjorth et al. 2005; Fox et al. 2005; Covino et al. 2006), (2) the first secure identification of the host galaxy, (3) the first secure measurement of the redshift ( $z = 0.16$ ) (Fox et al. 2005; Covino et al. 2006), and (4) the first determination of where in the host galaxy the burst occurred (Fox et al. 2005). No supernova light curve was detected in the case of either burst down to very sensitive limits (Fox et al. 2005).

The localization of GRB 050724 by Swift (Barthelmy et al. 2005a) also led to the detection of the X-ray (Barthelmy et al. 2005a) and optical (Berger et al. 2005a) afterglows

of the burst, a secure identification of the host galaxy, a determination of where in the galaxy the burst occurred, and a secure measurement of the redshift ( $z = 0.25$ ). The peak fluxes and fluences of GRBs 050709 and 050724, together with their redshifts, imply that these SPBs are a thousand times less luminous and energetic than are typical long GRBs.

Both bursts occurred in the outskirts of their host galaxies, implying that they come from very old systems, as do the facts that the host galaxy of GRB 050724 is an elliptical galaxy in which star formation ceased long ago and that no supernova light curve was detected in either case down to very sensitive limits. These results strongly support the interpretation that many SPBs are due to the mergers of neutron star-neutron star or neutron star-black hole binaries (Eichler et al. 1989; Narayan, Paczyński & Piran 1992), and are therefore likely associated with the emission of strong bursts of gravitational waves.

In contrast, “long population bursts” (LPBs) are known to have X-ray (Costa et al. 1997) and optical afterglows (van Paradijs 1997), to occur at cosmological distances (Metzger 1997) in star-forming galaxies (Castander & Lamb 1999), and to be associated with the explosion of massive stars (Stanek et al. 2003; Hjorth et al. 2003) .

HETE-2 has localized six short-duration GRBs so far. Observational results for HETE-2-localized short-duration bursts GRBs 020531 and 050709 have been reported previously (Lamb et al. 2004, 2006; Villasenor et al. 2005). In this paper, we report the results of HETE-2 observations of four other short-duration bursts localized by HETE-2: GRBs 010326B, 040802, 051211, and 060121. These four bursts have  $T_{90}$  durations in the Fregate 30-400 keV energy band of 1.90, 2.31, 4.25, and 1.97 sec, respectively, yielding probabilities  $P(S|T_{90}) = 0.97, 0.91, 0.60,$  and  $0.95$  that these bursts are SPBs on the basis of their  $T_{90}$  durations alone. All four bursts also have spectral lags consistent with zero. These results provide strong evidence that all four of these GRBs are SPBs.

We focus particular attention on GRB 060121, a bright short-duration burst for which both X-ray (Mangano et al. 2006a,b) and optical (Levan et al. 2006b; Postigo et al. 2006) afterglows were detected, and a probable host galaxy identified (Levan et al. 2006b). The light curve of GRB 060121 consists of a hard spike followed by a long, soft bump – features that are similar to those of the light curves of the short bursts GRBs 050709 (Villasenor et al. 2005) and 050724 (Barthelmy et al. 2005a), and are characteristic of many – perhaps all – SPBs, as analysis of BATSE (Lazzati, Ramirez-Ruiz & Ghisellini 2001; Connaughton et al. 2002; Norris & Bonnell 2006) and Konus (Frederiks et al. 2004) short bursts have shown. This provides additional strong evidence that GRB 060121 is an SPB. GRB 060121 exhibits strong spectral evolution in both the value of the low-energy spectral index  $\alpha$  and in the peak energy  $E_{\text{peak}}^{\text{obs}}$  of the spectrum in  $\nu F_{\nu}$ , and we find that this spectral evolution obeys the Amati et al. (2002) relation internally.

GRB 060121 is the first short GRB for which it has been possible to obtain a photometric redshift from the optical and NIR afterglow of the burst (Postigo et al. 2006). The results provide strong evidence that GRB 060121 lies at a redshift  $z > 1.5$  and most likely at a redshift  $z = 4.6$  (Postigo et al. 2006) [see also Levan et al. (2006b)], making this the first short burst for which a high redshift has been securely determined [the short burst GRB 050813 may also lie at high redshift (Berger 2005b)]. At either redshift, the inferred luminosity  $L$ , and isotropic-equivalent energy  $E_{\text{iso}}$ , are  $\sim 100$  times larger than those inferred for GRBs 050709 and 050724, and probably for GRB 050509B, and are similar to those of long GRBs; and the values of  $E_{\text{iso}}$  and  $E_{\text{peak}}^{\text{obs}}$  are consistent with the Amati et al. (2002) relation. However, adopting the jet opening angles derived from modeling of its afterglow the values of  $E_{\gamma}$  are  $3.0 \times 10^{49}$  ergs if  $z = 1.5$  and  $1.3 \times 10^{49}$  ergs if  $z = 4.6$ . These values are similar to those of the SPBs GRB 050709 and GRB 050724 and  $\sim 100$  times smaller than those of almost all other hard GRBs. They therefore provide additional evidence that GRB 060121 is a SPB.

HST observations (Levan et al. 2006b) have shown that the probable host galaxy of GRB 060121 is irregularly shaped and undergoing star formation. The location of GRB 060121 appears not to be coincident with the strongest star forming regions in the galaxy, which provides additional evidence that it is an SPB. Thus, when taken together, the properties of GRB 060121 make a very strong, although not conclusive case, that GRB 060121 is an SPB.

In §2, 3, 4 and 5, we describe the HETE-2 observations of the short-duration bursts, GRBs 010326B, 040802, 051211, and 060121, respectively. For each burst we report their localizations, temporal properties and spectral analyses, including time-resolved spectroscopy of GRB 060121. We used XSPEC version 11.3.2 (Arnaud 1996) for all spectral analyses presented here. In §6 we discuss ten criteria for determining whether a particular burst is an SPB or an LPB, consider the properties of the four short-duration bursts in the light of these criteria, and discuss the implications for the nature of these four bursts – especially GRB 060121. In §7 we present our conclusions.

## 2. Observations of GRB 010326B

GRB 010326B (trigger H1496) was one of the very first GRBs detected by HETE-2. The burst was detected by both Fregate (Atteia et al. 2003) and the WXM (Kawai et al. 2003), but it occurred before the availability of real-time optical aspect data. Consequently, analysis of the burst was carried out on the ground and a WXM localization was circulated about 5 hours after the trigger (Ricker et al. 2005). Table 1 details the localization time line and Figure 1a shows a skymap. No optical transient was detected in the WXM error box

(Price et al. 2005).

The initial GCN reported a duration of “about 4 seconds” for this burst (Ricker et al. 2005), but recent analysis finds a  $T_{90}$  duration in the 85-400 keV energy band of  $2.05 \pm 0.65$ . The duration of the burst increases at lower energies, reaching  $5.44 \pm 1.70$  in the 2-10 keV band (see Figure 6a and Table 2). An analysis of the spectral lag for this burst finds lag values of  $-4_{-32}^{+24}$  msec between the 40-80 keV and 80-400 keV bands, and  $-2_{-20}^{+16}$  msec between the 6-40 keV and 80-400 keV bands. Figure 2 shows the lightcurve of this burst in various energy bands.

Table 4 lists the results of the spectral analysis of this burst, which were first reported in Sakamoto et al. (2005a). The burst-average spectrum is well-fit by a power-law times an exponential (PLE)<sup>1</sup> model, with spectral index  $\alpha = -1.08_{-0.22}^{+0.25}$  and peak energy  $E_{\text{peak}}^{\text{obs}} = 51.8_{-11.3}^{+18.6}$  keV. A simple PL model is strongly disfavored. Fitting to a Band<sup>2</sup> model does not yield any decrease in  $\chi^2$  for the extra degree of freedom, and the high-energy PL index  $\beta$  is unconstrained by the fit. Table 6 gives the photon number and photon energy fluences, and the photon number and photon energy peak fluxes, in various energy bands for this burst. Figure 9 shows the best-fit PLE model and residuals for this burst.

As can be seen in Figure 17, the spectral properties of GRB 010326B make it the softest short event seen by HETE-2. However, this burst can be classified as a short GRB, based on its  $T_{90}$  duration and a spectral lag consistent with zero.

### 3. Observations of GRB 040802

GRB 040802 (trigger H3485) was a bright, short burst that was detected by Fregate but was only seen in the X-detector of the WXM. As is usual in such cases, we were able to obtain a narrow localization in the X-direction and a much wider localization in the Y-direction, derived from the exposure pattern in the X-detector. This resulted in a long, narrow localization that was reported in a series of GCN Notices. Table 1 details the localization time line and Figure 1b shows the skymap. The burst was also detected by the Mars Odyssey (HEND), Konus-Wind and INTEGRAL (SPI-ACS) instruments, and the IPN was

---

<sup>1</sup>Also known as a cutoff power-law, or CPL, model. It is defined by  $f(E) = A(E/E_{\text{scale}})^{\alpha} \exp(-E/E_0)$ , where  $E_0 = E_{\text{peak}}^{\text{obs}}/(2 + \alpha)$ . We take  $E_{\text{scale}} = 15$  keV for this work.

<sup>2</sup>The Band model (Band et al. 1993) is defined by  $f(E) = A(E/E_{\text{scale}})^{\alpha} \exp(-E/E_0)$  for  $E < E_{\text{break}}$  and  $f(E) = A(E_{\text{break}}/E_{\text{scale}})^{\alpha-\beta} \exp(\beta - \alpha)(E/E_{\text{scale}})^{\beta}$  for  $E \geq E_{\text{break}}$ , where  $E_0 = E_{\text{peak}}^{\text{obs}}/(2 + \alpha)$  and  $E_{\text{break}} = E_0(\alpha - \beta)$ . We take  $E_{\text{scale}} = 15$  keV for this work.

able to derive an annulus that intersected the WXM error box. The  $\sim 80$  square arcminute intersection was reported by Hurley et al. (2004). No afterglow has been reported for this burst.

GRB 040802 has a  $T_{90}$  duration in the 85-400 keV energy band of  $1.35 \pm 0.34$ . The duration of the burst increases at lower energies, reaching  $3.44 \pm 0.76$  in the 6-15 keV band (see Figure 6b and Table 2). An analysis of the spectral lag for this burst finds lag values of  $29^{+32}_{-30}$  msec between the 40-80 keV and 80-400 keV bands, and  $-6^{+15}_{-16}$  msec between the 6-40 keV and 80-400 keV bands. Figure 3 shows the lightcurve of this burst in various energy bands.

Table 4 lists the results of our spectral analysis of this burst. The burst is well-fit by a PLE model, with spectral index  $\alpha = -0.85^{+0.23}_{-0.20}$  and peak energy  $E_{\text{peak}}^{\text{obs}} = 92.2^{+18.8}_{-13}$  keV. A fit to a simple PL model is strongly disfavored. Fitting to a Band model does not yield any decrease in  $\chi^2$  for the extra degree of freedom, and the high-energy PL index  $\beta$  is unconstrained by the fit. Table 6 gives the photon number and photon energy fluences, and the photon number and photon energy peak fluxes, in various energy bands for this burst. Figure 10 shows the best-fit PLE model and residuals for this burst.

GRB 040802 can be classified as a short GRB, based on its  $T_{90}$  duration and a spectral lag consistent with zero. Its spectral properties are typical of those of HETE-2 short GRBs.

#### 4. Observations of GRB 051211

The short GRB 051211 was detected by the Fregate, WXM and SXC (Villasenor et al. 2003) instruments. A WXM flight localization with a correct X-location but an incorrect Y-location was sent out in near real time. Ground analysis of the WXM data confirmed the flight X position, but due to low signal-to-noise in the Y-detector, yielded three roughly equivalent Y position candidates. The SXC was able to localize soft emission occurring  $\sim 35$  seconds after the harder emission that triggered Fregate and the WXM. This emission yielded a SXC X position that matched the WXM X localization and a SXC Y position that matched one of the WXM Y candidates. This SXC localization was reported by Atteia et al. (2005) and confirmed by Kawai et al. (2005). Multiple follow-up observations yielded a possible optical counterpart (Guidorzi et al. 2005), that was later found to be more likely a star and not an afterglow (Halpern et al. 2005). Table 1 details the localization time line and Figure 1c provides a skymap.

GRB 051211 has a  $T_{90}$  duration in the 85-400 keV energy band of  $4.02 \pm 1.28$  seconds. The duration of the burst increases slightly at lower energies, reaching  $4.82 \pm 0.79$  in the 6-40



keV band (see Figure 6c and Table 2). A spectral lag of  $0 \pm 24$  msec between the 30-85 keV and 85-400 keV bands was first reported by Norris et al. (2005a). We have further calculated a spectral lag of  $-2 \pm 23$  msec between the 40-80 keV and 80-400 keV bands. Figure 4 shows the lightcurve of this burst in various energy bands.

Table 4 lists the results of our spectral analysis of this burst. The burst is well-fit by a PLE model, with spectral index  $\alpha = -0.07_{-0.41}^{+0.50}$  and peak energy  $E_{\text{peak}}^{\text{obs}} = 121_{-20.3}^{+33.0}$  keV. A fit to a simple PL model is strongly disfavored. Fitting to a Band model spectrum does not yield any decrease in  $\chi^2$  for the extra degree of freedom, and the high-energy PL index  $\beta$  is unconstrained by the fit. Table 6 gives the photon number and photon energy fluences, and the photon number and photon energy peak fluxes, in various energy bands for this burst. Figure 11 shows the best-fit PLE model and residuals for this burst.

GRB 051211 can be classified as a short GRB, based on its  $T_{90}$  duration and a spectral lag consistent with zero. Its spectral properties are typical of those of HETE-2 short GRBs.

## 5. Observations of GRB 060121

On January 21 2006, at 22:24:54.5 UTC (80694.5 SOD), HETE-2 detected a short GRB with Fregate. GRB 060121 was localized correctly in flight by the WXM and the position was relayed to the GCN burst alert network within 13 seconds after the start of the burst. The burst was also detected by the SXC, whose smaller error region was distributed after analysis of the data on the ground. Optical and X-ray transients were discovered in the SXC error box, thus placing this burst on the short list of short GRBs with observed afterglows. This burst has provided a wealth of new results about short GRBs which we outline in this section.

### 5.1. Localization

The WXM flight location of GRB 060121 (with the standard  $14'$  error radius) was relayed to the ground via the burst alert network 13 seconds after the start of the burst. After reviewing the data on the ground, a revised localization (Arimoto et al. 2006) with an  $8'$  radius was distributed 48 minutes after the trigger. The SXC position with a 90 % confidence error radius of  $80''$  was distributed 90 minutes after the trigger (Prigozhin et al. 2006).

The Swift satellite performed a 5 ksec ToO observation of the HETE-2 error box beginning on 22 January 2006 at 01:21:37 UTC, or 2hr 56min 42.5s after the HETE trigger.

Mangano et al. (2006a) reported a bright source inside the SXC error circle, located at R.A.  $+09^{\text{h}} 09^{\text{m}} 52.13^{\text{s}}$ , Dec  $+45^{\circ} 39' 44.9''$ , that was seen to fade in later observations (Mangano et al. 2006b). Early optical and infrared observations of the SXC error circle did not reveal any optical detections, however after the discovery of the bright X-Ray transient, two groups (Malesani et al. 2006; Levan et al. 2006a) reported detections of a very faint, variable optical source at the position of the XRT source in the previously reported observations. Detection of the near infrared (NIR) afterglow was reported by Hearty et al. (2006a,b), and further observations were reported for the afterglow (Postigo et al. 2006; Levan et al. 2006b) and the host galaxy (Levan et al. 2006b).

Table 1 details the time line of localizations by the WXM and SXC instruments, as well as the X-ray and optical followups. Figure 1d shows the relative sizes of the error regions for the WXM Flight, WXM Ground, and SXC Ground localizations, and the position of the optical and X-ray counterparts.

## 5.2. Temporal Properties

Figure 5 shows the light curve of GRB 060121 in various energy bands. The burst structure shows two peaks at  $\sim 2$  and  $\sim 3$  seconds after the trigger. GRB 060121 has a  $T_{90}$  duration in the 85-400 keV energy band of  $1.60 \pm 0.07$  seconds. Figure 6 and Table 2 show the dependence of  $T_{90}$  and  $T_{50}$  on energy. The duration of GRB 060121 is shorter at higher energies than at lower ( $T_{90} \approx 10$  sec in the 2-10 keV band), as is the case for the short burst GRB 020531 (Lamb et al. 2004, 2006), as well as most long bursts. The discrepancy between WXM and Fregate  $T_{90}$  durations in similar bands in Table 2 is due to the different background levels and sensitivities of the two instruments, and to the fact that  $T_{90}$  is highly sensitive to the choice of background. An analysis of the spectral lag for this burst finds lag values of  $2_{-14}^{+29}$  msec between the 40-80 keV and 80-400 keV bands, and  $17 \pm 9$  msec between the 6-40 keV and 80-400 keV bands.

Figures 7 and 8 show the light curves of GRB 060121 in the WXM 2-5 keV and 2-10 keV energy bands and the SXC 2-14 keV energy band from 50 s before the trigger until 300 s after the trigger, binned at  $\sim 1$  and  $\sim 3$  seconds respectively. Visual inspection of these light curves reveals evidence for a long, soft bump beginning about 70 s after the trigger and extending to about 120 s after the trigger in the WXM, and 150 s after the trigger in the SXC. To assess the significance of this soft bump, we compare two models using the likelihood ratio test, one assuming only a flat background is present and one assuming a flat background plus a constant emission lasting from  $t_1$  to  $t_2$  are present.

We find evidence for the presence of soft emission in the interval from  $t_1 = 66.87$  sec to  $t_2 = 155.43$  sec in the SXC 2-14 keV energy band at a significance level of  $4.4 \times 10^{-4}$ . We also find evidence for the soft emission from  $t_1 = 70$  sec to  $t_2 = 122$  sec in the WXM 2-5 keV and 2-10 keV energy bands at significance levels of 0.016 and 0.009, respectively. Thus the light curve of GRB 060121 consists of a spike plus a long, soft bump beginning about 70 seconds after the spike and lasting about 50-90 seconds.

### 5.3. Spectrum

Table 5 lists the results of our spectral analysis of this burst. The burst-average spectrum ( $t=0-10$  sec) of GRB 060121 is adequately fit by a PLE model, with spectral index  $\alpha = -0.79_{-0.11}^{+0.12}$  and peak energy  $E_{\text{peak}}^{\text{obs}} = 114_{-11}^{+14}$  keV (see the second-to-last set of entries in Table 5). A fit to a simple PL model is strongly disfavored. A fit to a Band model spectrum does not yield any increase in  $\chi^2$  for the extra degree of freedom, and the high-energy powerlaw index  $\beta$  is unconstrained by the fit. Figure 12 shows the comparison of the burst-average observed and predicted spectrum in count space. The best-fit parameter values that we find for a PLE model are consistent with the values of  $\alpha = -0.51_{-0.60}^{+0.55}$ , peak energy  $E_{\text{peak}}^{\text{obs}} = 134_{-17}^{+32}$  keV, and  $\beta = -2.39_{-1.41}^{+0.27}$ , reported by (Golenetskii et al. 2006a) for a Band model from a preliminary analysis of KONUS-WIND spectral data for the burst.

GRB 060121 was bright enough for us to perform a time-resolved spectral analysis of the burst. Preliminary results of our joint WXM and Fregate spectral analysis were reported by (Boer et al. 2006); the final results are summarized in Table 5.

Figure 13 shows the background and 5 foreground regions that we used for the time-resolved spectral analysis. We selected the following five time intervals for our spectral analysis:  $t = 0.0 - 1.75$ ,  $1.75 - 2.7$ ,  $2.7 - 3.64$ ,  $3.64 - 5.186$  and  $5.186 - 10.0$  seconds, as measured from the trigger time. The spectral data for each of the five time intervals are well fit by a PLE model (as were each of the 3 short GRBs considered above). In each case, a simple PL model is strongly disfavored and fitting to a Band model spectrum does not yield any decrease in  $\chi^2$  for the extra degree of freedom, nor is the high-energy PL index  $\beta$  constrained by the fit. Table 5 lists the results of our spectral analysis and Figure 14 shows the best-fit PLE model and residuals for each of the five time intervals. Table 5 also lists the results of our spectral analysis of the time intervals  $t = 1.75 - 3.64$ ,  $0.0 - 3.64$  and  $0.0 - 5.186$  sec. The Band spectral model is favored over the PLE model for the time interval  $t = 1.75 - 3.64$  sec as a consequence of the rapid spectral evolution that is occurring within it.

We have calculated the 68% confidence region in the  $[\alpha, E_{\text{peak}}^{\text{obs}}]$ -plane for each time interval. Figure 15 shows the dramatic spectral evolution of the burst from a soft spectrum with a low  $E_{\text{peak}}^{\text{obs}}$  during the rise of the first peak, to a quite hard spectrum with a high  $E_{\text{peak}}^{\text{obs}}$  during the first peak, followed by softening and a decrease in  $E_{\text{peak}}^{\text{obs}}$  during the second peak and into the tail. Liang, Dai & Wu (2004) showed that the time-resolved spectra of bright BATSE long bursts obeys internally the  $E_{\text{peak}} - L$  relation found by (Yonetoku, et al. 2004) [see also Lamb, Donaghy, & Graziani (2005)]. Following Liang, Dai & Wu (2004), in Figure 16, we plot  $E_{\text{peak}}^{\text{obs}}$  against the average energy flux in each time interval and find that the four points are consistent with a slope of +2, as is the case for long GRBs.

We have also analyzed the spectrum of the long, soft bump seen in the WXM 2-5 keV and 2-10 keV time history data. The WXM 3-25 keV spectral data in the time interval  $t = 71.2 - 121.6$  sec as measured from the trigger time (which matches as closely as we can the time interval during which soft emission is present, identified above) is adequately fit by a simple PL spectrum with a PL index  $\alpha = -2.81_{-2.11}^{+1.14}$  (see Table 5). The lower right panel of Figure 14 shows the count spectrum and the residuals for the fit to the WXM data.

## 6. Discussion

Observations of short-duration GRBs, especially GRBs 050709 and 050724, made last summer by HETE-2 and Swift provide strong evidence that some short-duration GRBs come from merging neutron star-neutron star or neutron star-black hole binaries, whereas it has been known for some time that most long-duration GRBs come from the collapse of massive stars. However, as we will discuss below, there are clearly “short” GRBs (i.e., bursts that almost certainly come from the merger of compact binaries) with durations at least as long as 8 s, and “long” GRBs (i.e., bursts that come from the collapse of massive stars) with durations at least as short as  $\sim 2$  s. Thus, a given “short” burst can be longer than many “long” bursts, and a given “long” burst can be shorter than many “short” bursts, making this nomenclature quite awkward.

Another possibility might be to classify bursts as “merger,” “magnetar,” or “collapsar” GRBs, since the nature of the central engine that produces each kind of burst is key. However, it seems premature to try to assign bursts to these three classes at this time.

Therefore, in this paper, we adopt the terms “short population burst” (SPB) and “long population burst” (LPB). These terms have the advantage of being closely related to the often-used terms “short burst” and “long burst,” while emphasizing that reference is being made to two different *populations* of bursts, many of whose attributes overlap. We note that

there is some evidence from the distribution of BATSE bursts in duration and hardness for a third population of soft bursts with durations intermediate between those of SPB and LPB bursts (Horváth 1998, 2002; Horváth et al. 2006). How this third population of bursts, if it exists, relates to the GRBs produced by the merger of compact binaries or the collapse of massive stars, is unknown.

In this section, we first discuss ten criteria for determining whether a particular burst is an SPB or a LPB. We then consider the temporal and spectral properties of three of the HETE-2 short-duration bursts described in detail in this paper, in the light of four of these ten criteria. We then discuss in detail the properties of the fourth burst, GRB 060121, and consider these properties in the light of all ten criteria. Finally, we consider the properties of eight HETE-2 short-duration GRBs and twelve Swift short-duration GRBs observed to date in the light of these ten criteria.

### 6.1. Criteria for Distinguishing Between SPBs and LPBs

We consider ten criteria for determining whether a particular burst is an SPB or a LPB. These criteria are (1) duration, (2) pulse widths, (3) spectral hardness, (4) spectral lag, (5) energy  $E_\gamma$  radiated in gamma rays (or equivalently, the kinetic energy  $E_{\text{KE}}$  of the GRB jet), (6) existence of a long, soft bump following the burst, (7) location of the burst in the host galaxy, (8) lack of detection of a supernova component to deep limits, (9) type of host galaxy and (10) detection of gravitational waves.

The redshift distribution of the SPBs observed by HETE-2 and Swift is uncertain, but possibly broad; the redshift distribution of LPBs is certainly broad. This broadens the distributions of the properties of the bursts themselves, weakening the power of the first four above criteria to distinguish between SPBs and LPBs. It would therefore be preferable – from both an empirical and a theoretical point of view – to apply these criteria to the properties of the bursts themselves, as measured in the rest frame of the burst. However, this would limit the application of these criteria to bursts whose redshifts are known, which is a small fraction of both populations of bursts. Worse, it is difficult to determine the necessary burst properties in the rest frame of the burst, and in the case of some properties, it is impossible to do so, as we discuss below. Therefore, in this paper, we apply the criteria to the properties of the bursts themselves as measured in the observer frame.

The temporal properties of SPBs differ from those of LPBs in two ways: SPBs generally have shorter durations than do LPBs and the time histories of SPBs generally have much narrower pulses than do LPBs (Lamb, Graziani & Smith 1993; Norris et al. 1994, 1996), as

benefits both, given the nomenclature for the two populations that we use in this paper. These two differences in temporal properties can potentially be used to distinguish between SPBs and LPBs.

The  $T_{50}$  duration distribution of GRBs exhibits two peaks that strongly overlap. These two peaks are more evident in the  $T_{90}$  duration distribution (Hurley 1992; Lamb, Graziani & Smith 1993; Kouveliotou et al. 1992), but  $T_{90}$  is more difficult to measure. The peaks in the  $T_{90}$  distribution lie at  $T_{90} \approx 0.3$  s and  $T_{90} \approx 30$  s, and the minimum in between lies at  $T_{90} \approx 2$  s. The double-peaked  $T_{90}$  duration distribution can be well fit by two (or three) lognormal distributions [see, e.g., (Horváth 1998, 2002; Horváth et al. 2006)]. However, observational selection effects may affect both the  $T_{50}$  and the  $T_{90}$  duration distributions. As one example, the short end of the duration distribution very likely reflects the fact that the shortest BATSE trigger was 64 ms, rather than the intrinsic duration distribution of SPBs (Lee & Petrosian 1996).

Determining the  $T_{50}$  and  $T_{90}$  durations of GRBs in the rest frame of the burst would require taking into account three factors: (1) cosmological time dilation, which is proportional to  $1 + z$ ; (2) the dependence of the duration on the energy band in which it is measured, which is approximately proportional to  $(1 + z)^{-0.4}$ , and (3) the fact that  $T_{50}$  and  $T_{90}$  depend on the background level. The first factor is straightforward to account for. The second can be accounted for either approximately by using the factor  $(1 + z)^{-0.4}$ , which is correct on average, or by attempting to measure the  $T_{50}$  and  $T_{90}$  durations in a fixed energy band in the rest frame of the burst – something that is difficult to do, given the possible broad redshift range of SPBs and the known broad redshift range of LPBs. The third is impossible to account for, since it would require knowing the light curve of the burst far below the level of the background (i.e., with essentially infinite accuracy). In another paper, we explore the use of the distribution of the “emission duration” introduced by Reichart et al. (2001) as a possible criterion for distinguishing between SPBs and LPBs (Donaghy, Graziani, & Lamb 2006). Unlike  $T_{50}$  or  $T_{90}$  durations, the “emission duration” can be defined in the rest frame of the burst.

In the present paper, we restrict ourselves to the use of  $T_{90}$  as a criterion for distinguishing between SPBs and LPBs. Using the best-fit parameters for the fit to the  $T_{90}$  duration distribution carried out by Horváth (2002) for two lognormal distributions, we have developed a likelihood method for determining the probability that a burst is an SPB or a LPB on the basis of its  $T_{90}$  duration alone (Donaghy, Graziani, & Lamb 2006). Figure 18 shows the resulting probability distribution. A striking feature of the resulting probability distribution is that the  $T_{90}$  duration at which a burst has an equal probability of being a SPB or a LPB is  $T_{90} = 5$  s. The reason is that the duration distribution of SPBs is very broad ( $\log \sigma = 0.61$ ).

Thus, the appropriate duration to use in dividing bursts into SPBs and LPBs is  $T_{90} = 5$  s, *not*  $T_{90} = 2$  s, which is the criterion that is often used to separate the two populations.

Pulse widths in SPBs are much smaller than those in LPBs (Lamb, Graziani & Smith 1993; Norris et al. 1994, 1996). The pulse width distribution in SPBs has a mean of  $\sim 60$  ms, while that for LPBs has a mean of  $\sim 600$  ms (Norris et al. 1994, 1996). However, both distributions are broad. Therefore, pulse widths provides a good, but not conclusive, criterion for distinguishing whether a particular burst is an SPB or a LPB.

The spectral properties of SPBs also differ from those of LPBs in two ways: the distribution of hardness ratios for SPBs may be somewhat harder than the distribution of hardness ratios for LPBs; and, at high energies, SPBs exhibit zero spectral lag (Norris & Bonnell 2006), whereas all LPBs for which a spectral lag has been measured exhibit non-zero spectral lag (Norris 2002). These two differences in spectral properties can potentially be used to distinguish between SPBs and LPBs.

SPBs have often been said to be harder than LPBs [see, e.g., (Kouveliotou et al. 1992)]. However, the distributions of the hardness ratios for the two populations are broad and overlap greatly, making it difficult to use this criterion to distinguish between SPBs and LPBs. In addition, Sakamoto et al. (2006) has recently shown that the short and long GRBs detected by KONUS-WIND appear to have very similar hardness ratios. Figure 17 shows that the hardness ratios for SPBs and for the hardest LPBs localized by HETE-2 and by Swift are also very similar (Sakamoto et al. 2006). Furthermore, it is clear from Figure 17 that observational selection effects can strongly affect the hardness ratio distributions, since the BATSE sample of GRBs is missing many of the X-ray-rich GRBs and all of the XRFs localized by HETE-2. All of these properties make the hardness ratio a difficult criterion to use to distinguish between SPBs and LPBs. Therefore, we do not use this criterion.

Extensive studies have shown that, at high energies, SPBs exhibit zero spectral lag (Norris & Bonnell 2006), whereas all LPBs for which a spectral lag has been measured exhibit non-zero spectral lag (Norris 2002)<sup>3</sup>. We therefore consider an accurate measurement of spectral lag, if it can be done, to be one of the best criteria for distinguishing between SPBs and LPBs.

The spectral lag measurements for a number of the HETE-2 short-duration GRBs have relatively large uncertainties, making it difficult to reach definite conclusions about whether

---

<sup>3</sup>We note that zero spectral lag does not preclude strong spectral evolution during a burst, if the burst consists of more than one peak and the peaks have different spectral properties. What it does preclude is strong spectral evolution within each peak.

these bursts are SPBs or LPBs on the basis of spectral lag alone. In another paper, we explore the use of spectral lag measurements as a means of distinguishing between SPBs and LPBs, using the model of the spectral lag distribution for LPBs developed by Norris (2002) and taking into account rigorously the uncertainty in the measurement of spectral lag (Donaghy, Graziani, & Lamb 2006).

The energy  $E_\gamma$  radiated by a burst in gamma rays is  $E_\gamma = 10^{48} - 10^{49}$  ergs for the SPBs GRB 050709, and 050724, and  $E_\gamma \sim 10^{50} - 10^{51}$  ergs for *hard* LPBs. We therefore consider  $E_\gamma$  to be a good, but not conclusive, criterion for distinguishing between SPBs and LPBs.

Long, soft bumps were seen in the light curves of the short bursts GRBs 050709 (Villasenor et al. 2005) and 050724 (Barthelmy et al. 2005a), and appear to be characteristic of many – perhaps all – SPBs, as analysis of BATSE (Lazzati, Ramirez-Ruiz & Ghisellini 2001; Connaughton et al. 2002; Norris & Bonnell 2006) and Konus (Frederiks et al. 2004) short bursts have shown. We therefore consider the existence of a long, soft bump to be one of the best criteria for distinguishing between SPBs and LPBs.

The precise localizations made possible by detection of the optical afterglows (Hjorth et al. 2005; Fox et al. 2005; Covino et al. 2006; Berger et al. 2005a) of the short bursts GRBs 050709 (Villasenor et al. 2005) and 050724 (Barthelmy et al. 2005a) revealed that both bursts occurred in the outskirts of their host galaxies. In addition, no supernova light curve was detected in either case down to very sensitive limits (Fox et al. 2005; Berger et al. 2005a). These results provide strong support for the interpretation that many short GRBs are due to the mergers of neutron star-neutron star or neutron star-black hole binaries (Eichler et al. 1989; Narayan, Paczyński & Piran 1992). In contrast, every LPB for which an accurate location has been determined is coincident with a bright star-forming region in the host galaxy (Fruchter et al. 2006); indeed, the locations of LPBs are much more tightly concentrated in these star-forming regions than is the blue light from the host galaxy. We therefore consider the location of the burst to be one of the best criteria for distinguishing between SPBs and LPBs.

Supernova components have been detected in the optical afterglow light curves of many LPBs, and are a common feature in the optical afterglow light curves of LPBs that lie at redshifts  $z < 1$ . In contrast, supernova light curves are not expected for SPBs that come from the mergers of compact binaries, and none were detected to very deep limits for GRB 050509b and GRB 050709 (Fox et al. 2005). We therefore consider the presence or absence of a supernova component in the optical afterglow light curve to be one of the best criteria for distinguishing between SPBs and LPBs. In particular, we regard the clear detection of a supernova component to be very strong evidence that the burst is an LPB, and the lack of detection of a supernova component down to deep limits to be very strong evidence that



the burst is an SPB, provided that the burst lies at a redshift  $z < 1$ .

The SPB GRB 050724 occurred in an elliptical galaxy (Barthelmy et al. 2005a; Berger et al. 2005a) in which star formation ceased long ago, as probably did GRB 050509b Gehrels et al. (2005). However, two other SPBs [GRB 050709 (Villasenor et al. 2005) and GRB 051221A (Berger & Soderberg 2005)] occurred in star-forming galaxies (Hjorth et al. 2005; Fox et al. 2005; Covino et al. 2006; Soderberg et al. 2006). Indeed, even in some cases where the host galaxy cannot be identified, it may be sufficient to demonstrate that the stellar population is old, as Gorosabel et al. (2006) argue for the case of 050813. We therefore consider that, if a particular burst occurs in an elliptical galaxy, this is conclusive evidence that it is an SPB, while if the burst occurs in a star-forming galaxy, the kind of host galaxy provides no information about whether the burst is an SPB or an LPB.

If most SPBs are indeed due to mergers of neutron star-neutron star or neutron star-black hole binaries, these events produce powerful bursts of gravitational radiation (Eichler et al. 1989; Narayan, Paczyński & Piran 1992) that should be detectable by the second-generation Laser Interferometry Gravitational-wave Observatory (Thorne & Cutler 2002; Belczynski et al. 2006). The detection of gravitational waves from a short-duration GRB would therefore provide conclusive evidence that the event is an SPB. While it is unlikely that gravitational waves will be detected from a short-duration GRB anytime soon, the detection of such waves will eventually be the gold standard for determining whether a burst is an SPB, and we therefore include it here.

In summary, we have discussed ten possible criteria for determining whether a particular burst is an SPB or a LPB. Based on a careful consideration of the strengths and weaknesses of each of the criteria, we rate spectral lag; long, soft bump; location in the host galaxy; type of host galaxy; and detection of gravitational waves as “gold” criteria (i.e., the best criteria); duration, pulse width, and  $E_\gamma$  as “silver” criteria (i.e., good criteria), and spectral hardness as a “bronze” criterion (i.e., a poor criterion).

## 6.2. Temporal Properties

In this section, we consider the temporal properties of the four HETE-2 short-duration bursts discussed in detail in this paper in the light of criteria (1-2) discussed above.

Table 8 shows that three of the four bursts have probabilities  $P(S|T_{90}) > 0.9$  of being SPBs, based on their  $T_{90}$  durations alone, and that in the cases of GRBs 010326B and 060121, the probability is 0.95 or greater. The table shows that  $P(S|T_{90}) > 0.85$  for four HETE-2 short bursts (GRBs 020531, 021211, 040924, and 050709) whose properties have

been reported elsewhere (Lamb et al. 2004, 2006; Crew, et al. 2003; Fenimore, et al. 2004; Villasenor et al. 2005), and GRBs 020531 and 050709 have probabilities 0.995 and 1.000 of being SPBs, based on their  $T_{90}$  durations alone.

A detailed analysis of the pulse widths of the four HETE-2 short GRBs discussed in detail in this paper and a quantitative comparison of these widths with the pulse width distributions of SPBs and LPBs lies beyond the scope of the present paper. However, we are particularly interested in GRB 060121. We have therefore made very rough estimates of the widths of the three pulses that are most clearly evident in this burst. These three pulses have FWHMs of 600-800 ms, 300-400 ms, and 300-500 ms in the observer frame. These pulse widths are larger than is typical of SPBs and somewhat smaller than is typical of LPBs; consequently, the widths of the pulses in GRB 060121 considered in the observer frame provide no clear evidence one way or another about whether the burst is an SPB or a LPB. However, pulse widths (unlike  $T_{50}$  and  $T_{90}$  durations) can be calculated in the rest frame of the burst, and we revisit these pulse widths below, after having discussed the redshift of GRB 060121.

### 6.3. Spectral Properties

In this section, we consider the spectral properties of the four HETE-2 short-duration bursts discussed in detail in this paper in light of criteria (3-4) discussed above.

The burst-average spectra of the four HETE-2 short GRBs discussed in this paper are characterized by low-energy spectral indices  $\alpha = 0.07_{-0.41}^{+0.50} - 1.08_{-0.22}^{+0.25}$  and peak energies  $E_{\text{peak}}^{\text{obs}} = 51.8_{-11.3}^{+18.6} - 121_{-20.3}^{+33.0}$ . Similar values were found for the two HETE-2 short GRBs whose spectral properties were reported elsewhere (Lamb et al. 2004, 2006; Villasenor et al. 2005). The values of  $\alpha$  and  $E_{\text{peak}}^{\text{obs}}$  for the six HETE-2 short GRBs are typical of those for bright short GRBs detected by BATSE (Ghirlanda et al. 2004) and for the three short GRBs localized by Swift for which a PLE model is requested by the Swift BAT spectral data (see Table 8). We note that in none of the six HETE-2 short GRBs do the spectral data request a Band model; this is also the case for bright short GRBs detected by BATSE (Ghirlanda et al. 2004).

As already reported, we have calculated the spectral lag for the four HETE-2 short-duration GRBs discussed in detail in this paper. We have also calculated the spectral lag for four other HETE-2 short-duration GRBs. Table 3 shows that the spectral lags measured for six of these eight HETE-2 short GRBs are consistent with zero, taking into account the uncertainty in the measurement, and that in two cases (GRBs 020531 and 050709) the

upper limit on any spectral lag is very small. However, Table 3 also shows that the remaining two HETE-2 short-duration bursts (GRBs 021211 and 040924) exhibit definite spectral lags. These two bursts are therefore LPBs, despite the fact that their  $T_{90}$  durations are only 2.7 s and 2.4 s and the probabilities that they are SPBs are 0.87 and 0.90, respectively, on the basis of their  $T_{90}$  durations alone (see Table 8). The results for these two bursts illustrate the difficulty in determining whether a given burst belongs to either the short or the long classes of GRBs, using solely its  $T_{90}$  duration, and the ability of a spectral lag analysis to do so (Norris & Bonnell 2006).

#### 6.4. Properties of GRB 060121

The light curve of GRB 060121 consists of a hard spike followed by a long, soft bump, and in this way, it is similar to those of the SPBs GRB 050709 (Villasenor et al. 2005) and GRB 050724 (Barthelmy et al. 2005a). These general features may well be typical of all SPBs seen by BATSE (Lazzati, Ramirez-Ruiz & Ghisellini 2001; Connaughton et al. 2002) and Konus (Frederiks et al. 2004). However, the ratio of the fluence in the burst itself and the fluence in the long, soft bump spans a range of at least  $10^4$  (Norris & Bonnell 2006).

The photon number and photon energy fluences of GRB 060121 are more than twice those of any of the other four HETE-2 short GRBs discussed in this paper or of the other two HETE-2 short GRBs whose properties were reported elsewhere (Lamb et al. 2004, 2006; Villasenor et al. 2005). The large photon number and photon energy fluences of GRB 060121 have allowed us to perform time-resolved spectroscopy of this burst. We find that the spectrum of GRB 060121 exhibits dramatic spectral evolution in both the value of the low-energy spectral index  $\alpha$  and the value of the peak energy  $E_{\text{peak}}^{\text{obs}}$  of the spectrum in  $\nu F_{\nu}$  (see Table 5 and Figure 14). GRB 020531 also showed evidence for modest spectral evolution, but only in the value of its low-energy power-law index  $\alpha$  (Lamb et al. 2004, 2006). GRB 060121 is one of only a few short GRBs for which strong spectral evolution has been established.

Both the X-ray afterglow (Mangano et al. 2006a,b) and near infrared (NIR) afterglow (Hearty et al. 2006a,b) of GRB 060121 were bright, but the optical afterglow was faint (Malesani et al. 2006; Levan et al. 2006a; Breeveld et al. 2006). Nevertheless, at early times the afterglow was much brighter than the probable host galaxy (Levan et al. 2006b) in both the optical and the NIR. GRB 060121 is consequently the first short GRB for which it has been possible to obtain a photometric redshift from the optical and NIR afterglow of the burst (Postigo et al. 2006). Observations of the afterglow in the I-, R-, and K-bands and the upper limits derived for the U-, B-, and V-bands indicate that the burst occurred at a

redshift  $z = 4.6 \pm 0.6$ , or less probably, at a redshift  $z = 1.5 \pm 0.2$  and with a large extinction ( $A_V = 1.4 \pm 0.4$ ) (Postigo et al. 2006).

Further support for a high redshift comes from the unusually red color of the probable host galaxy and the presence nearby on the sky of five extremely red objects (EROs), which are exceptionally faint (and therefore have low surface brightnesses) or are undetected in the *Hubble Space Telescope* (HST) ACS/F606W filter, but are relatively bright in the HST NICMOS F160W filter (Levan et al. 2006b). The five nearby EROs correspond to an overdensity on the sky of a factor of 20 (Levan et al. 2006b), suggesting that the host galaxy of GRB 060121 may belong to a cluster.

These results provide strong evidence that GRB 060121 lies at a redshift  $z > 1.5$ , and most likely at a redshift  $z = 4.6$  (Postigo et al. 2006) [see also Levan et al. (2006b)], making this the first SPB for which a high redshift has been securely determined.<sup>4</sup>

The  $T_{90}$  duration of the spike in the light curve of GRB 060121 is 1.97 s in the 30-400 keV energy band, which gives a probability of  $P(S|T_{90}) = 0.95$  of GRB 060121 being a SPB, based on its  $T_{90}$  duration alone. The spectral lag measurement for the spike in the time history of GRB 060121 is  $2_{-14}^{+29}$  ms between the 40-80 keV and 80-400 keV bands, which is consistent with zero spectral lag. These results provide very strong evidence that GRB 060121 is a classical short GRB.

The inferred peak luminosity  $L_{\text{iso}}$  and isotropic-equivalent energy  $E_{\text{iso}}$  of GRB 060121 are  $4.2 \times 10^{52}$  ergs  $\text{s}^{-1}$  and  $3.7 \times 10^{52}$  ergs (assuming  $z = 1.5$ ), or  $6.9 \times 10^{53}$  ergs  $\text{s}^{-1}$  and  $2.4 \times 10^{53}$  ergs (assuming  $z = 4.6$ ). These values are  $\sim 10$ -100 times larger than those inferred for the short GRBs 050709 and 050724, and probably GRB 050509B, and are similar to those of long GRBs. Modeling of the afterglow gives opening angles of  $2.3^\circ$  if  $z = 1.5$  and  $0.6^\circ$  if  $z = 4.6$ , although the uncertainties in the opening angles are substantial (Postigo et al. 2006). Taking these opening angles at face value implies that the energy  $E_\gamma$  in gamma-rays emitted by GRB 060121 is  $3.0 \times 10^{49}$  ergs if  $z = 1.5$  and  $1.3 \times 10^{49}$  ergs if  $z = 4.6$ . These values of  $E_\gamma$  are similar to those of the SPBs GRB 050709 and GRB 050724.

Figure 19 shows that the location of GRB 060121 in the  $(E_{\text{iso}}, E_{\text{peak}})$ -plane is consistent with the Amati et al. (2002) relation. In contrast, GRB 050709 lies well away from the Amati et al. (2002) relation, as do the trajectories of three of the other four HETE-2 short GRBs. However, with so few SPBs having measured spectral properties and redshifts, it is impossible to know whether this is evidence that GRB 060121 is not a SPB, or that SPBs

---

<sup>4</sup>The short burst GRB 050813 may also lie at high redshift, but no photometric or spectroscopic redshift of the host galaxy has been reported as yet (Berger 2005b).

form a broad swath in the  $(E_{\text{iso}}, E_{\text{peak}}^{\text{obs}})$ -plane, the upper end of which is consistent with the Amati et al. (2002) relation.

### 6.5. Nature of GRB 060121

In this section, we consider the properties of GRB 060121 in the light of nine of the ten criteria for determining whether a particular burst is an SPB or a LPB discussed above. Excepting the detection of gravitational waves, the nine criteria are (1) duration, (2) pulse widths, (3) spectral hardness, (4) spectral lag, (5) energy  $E_\gamma$  radiated in gamma-rays (or equivalently, the kinetic energy  $E_{\text{KE}}$  of the GRB jet), (6) existence of a long, soft bump following the burst, (7) location of the burst in the host galaxy, (8) lack of detection of a supernova component to deep limits and (9) type of host galaxy.

*Duration.* The  $T_{90}$  duration of GRB 060121 in the 30-400 keV energy band is 1.97 s, which gives a probability of  $P(S|T_{90}) = 0.95$  of GRB 060121 being a SPB, based on its  $T_{90}$  duration alone. Furthermore, assuming that the light curve of the burst has no low-level peaks that are masked by the background, the  $T_{90}$  duration of the burst would be 0.8 s (if  $z = 1.5$ ) and 0.3 s (if  $z = 4.6$ ) if it had occurred at  $z = 1.2$ , a redshift similar to those at which GRBs 050709 ( $z = 1.17$ ) and 0507024 ( $z = 1.25$ ) occurred, where we have taken into account cosmological time dilation but neglected the dependence of burst duration on the energy band, since the burst is comprised of at least three peaks. Thus, criterion (a) provides strong evidence that GRB 060121 is a SPB.

*Pulse Width.* The widths of the three pulses visible in the time history of GRB 060121 are roughly 600-800 ms, 300-400 ms, and 300-500 ms in the observer frame. These pulse widths would be 300-400 ms, 150-200 ms, and 150-250 ms (assuming  $z = 1.5$ ) and 130-170 ms, 60-90 ms, and 60-110 ms (assuming  $z = 4.6$ ) if GRB 060121 had occurred at  $z = 1.2$ , a redshift similar to those at which GRBs 050709 and 0507024 occurred. Thus, if  $z = 1.5$ , the pulse widths are a factor of a few larger than those typical of SPBs and a factor of a few smaller than those typical of LPBs; the application of criterion (2) is therefore inconclusive. However, if  $z = 4.6$ , the pulse widths are similar to those of SPBs and much smaller than those of LPBs; the application of criterion (1) then provides evidence that GRB 060121 is a SPB.

*Spectral Hardness.* As discussed above, it is very difficult to use spectral hardness as a criterion for distinguishing between SPBs and LPBs. We therefore do not use this criterion.

*Spectral Lag.* The spectral lag measurement for the spike in the time history of GRB 060121 is  $2_{-14}^{+29}$  ms between the 40-80 keV and 80-400 keV bands, which is consistent with

zero spectral lag, taking into account the uncertainty in the measurement. However, the uncertainty in the measurement is relatively large. Consequently, although the spectral lag measured for GRB 060121 is fully consistent with its being a SPB, the measurement provides only modest evidence that it is one.

*Energy Radiated in Gamma Rays.* Adopting the jet opening angles derived from fits to the afterglow light curve (Postigo et al. 2006) implies that the energy  $E_\gamma$  in gamma-rays emitted by GRB 060121 is  $3.0 \times 10^{49}$  ergs if  $z = 1.5$  and  $1.3 \times 10^{49}$  ergs if  $z = 4.6$ . These values of  $E_\gamma$  are similar to those of the SPBs GRB 050709 and GRB 050724 and much smaller than almost all *hard* GRBs. Thus, this criterion (5) provides strong evidence that GRB 060121 is a SPB.

*Existence of Long, Soft Bump.* GRB 060121 clearly exhibits a long, soft bump. Such a feature appears to be characteristic of all SPBs, although the ratio of the fluence in the long, soft bump and that in the sharp spike ranges over a factor of at least  $10^4$  (Norris & Bonnell 2006). Thus, this criterion (6) also provides strong evidence that GRB 060121 is a SPB.

*Location of Burst in Host Galaxy.* While the HST images of the probable host galaxy of GRB 060121 are noisy, the location of the burst appears not to be coincident with the strongest star forming regions in the galaxy, which provides evidence that it is an SPB.

*Supernova Light Curve.* No supernova component was detected in the optical afterglow light curve of GRB 060121; however, the detection of such a component is not expected, given that the burst lies at a redshift  $z > 1.5$ . Therefore, the failure to detect a supernova component provides no evidence about whether the burst is an SPB or an LPB.

*Type of Host Galaxy.* The probably host galaxy of GRB 060121 is a star-forming galaxy, and thus provides no evidence about whether the burst is an SPB or an LPB.

In summary, all of the properties of GRB 060121 are consistent with its being a SPB. Two criteria (pulse width and location of burst in host galaxy) provide modest evidence that it is a SPB, while three criteria ( $T_{90}$  duration;  $E_\gamma$ ; presence of a long, soft bump) provide strong evidence that it is a SPB. These results are summarized in Table 9. These results, taken together, provide very strong, but not conclusive, evidence that GRB 060121 is an SPB.

## 6.6. HETE-2 and Swift Short-Duration GRBs in Light of Ten Criteria for Distinguishing Between SPBs and LPBs

Table 8 lists some temporal and spectral properties of twenty short-duration bursts (eight HETE-2 short-duration bursts and the twelve Swift short-duration bursts observed so far), while Table 9 summarizes the evidence that these bursts are SPBs or LPBs in light of the nine of the ten criteria discussed above.

Table 8 shows that there is compelling evidence that GRBs 020531 and 050709 are SPBs on the basis of their  $t_{90}$  duration *and* their lack of any spectral lag. In the case of GRB 050709, the additional criteria involving its pulse width; the presence of a long, soft bump; its  $E_\gamma$ ; its location in the outskirts of its host galaxy; and the lack of a supernova component in its optical afterglow light curve, together with its  $t_{90}$  duration and the lack of any spectral lag, provide overwhelming evidence that this burst is an SPB.

Table 8 provides strong evidence that three of the four HETE-2 short-duration bursts discussed in this paper (i.e., GRBs 010326B, 040802, and 060121) are SPBs on the basis of their  $t_{90}$  duration alone, and that there is evidence that GRB 060121 is an SPB, if its redshift is  $z = 4.6$ . GRB 010326B is more likely to be an LPB than an SPB on the basis of its pulse widths. Table 9 shows that, in the cases of the short-duration bursts GRBs 010326B, 040802, and 051211, the information needed to apply the other six criteria is lacking. However, it is also important to note that in none of these three cases is there any evidence that supports their being LPBs.

Table 3 also shows that GRBs 021211 and 040924 exhibit definite spectral lags. These two bursts are therefore LPBs, despite the fact that their  $T_{90}$  durations are only 2.7 s and 2.4 s and the probabilities that they are SPBs are 0.87 and 0.90, respectively, on the basis of their  $T_{90}$  durations alone (see Table 8). As already commented above, the results for these two bursts illustrate the difficulty in determining whether a given burst belongs to either the short or the long classes of GRBs, using solely its  $T_{90}$  duration, and the ability of a spectral lag analysis to do so (Norris & Bonnell 2006). The existence of two LPBs whose  $T_{90}$  durations are  $\sim 1$  s in the rest frame of the burst would also appear to impose a severe constraint on the collapsar model of SPBs Woosley (1993); Zhang, Woosley, & MacFadyen (2003).

Table 8 shows that nine of the twelve short bursts localized by Swift so far have probabilities  $> 0.95$  of being SPBs, based on their  $T_{90}$  durations alone (the exceptions being GRBs 050724, 051227, and 060505). The table also shows that there is compelling evidence that nine of the twelve Swift short-duration bursts observed so far are SPBs on the basis of their lack of any spectral lag (the exceptions being GRB 051210 for which the uncertainty

in the spectral lag measurement is relatively large, and GRBs 050202 and 060505 for which spectral lag measurements have not yet been reported). There is thus compelling evidence that at least ten of the twelve Swift short-duration bursts observed so far are SPBs, the two exceptions being GRB050202 and GRB 060505 for which spectral lag measurements have not yet been reported.

Table 9 shows that, in the cases of the Swift short-duration bursts GRBs 050202, 050509b, 050813, 050906, 051105a, and 060502b, there is additional strong evidence that they are SPBs on the basis of their pulse widths. The table also shows that, in the cases of GRBs 050724 and 051227, there is additional compelling evidence that they are SPBs on the basis of the presence of a long, soft bump; in the cases of GRBs 050724 and 051221a, there is additional compelling evidence that they are SPBs on the basis of the location in the burst in its host galaxy; and in the cases of GRBs 050509b and 060505, there is additional compelling evidence that they are SPBs on the basis of the lack of a supernova component in its optical afterglow, down to deep limits.

Considering all of the evidence together, we consider that – of the eight HETE-2 short-duration bursts discussed in this paper – there is conclusive evidence that two are SPBs (GRBs 020531 and 050709), there is very strong but not conclusive evidence that a third is an SPB (GRB 060121), and there is moderately strong evidence that three others are SPBs (GRBs 010326b, 040802, and 051211). Finally, there is conclusive evidence that the remaining two bursts are LPBs (GRBs 021211 and 040924). We also consider that – of the twelve Swift short-duration bursts discussed in this paper – there is conclusive evidence that three are SPBs (GRBs 050509b, 050724, 051227); compelling evidence that seven of the remaining nine bursts are SPBs; and moderately strong evidence that one of the two remaining bursts is an SPB, the sole exception being GRB 050202 for which very little information has been reported.

## 7. Conclusions

In this paper, we have reported the localizations and observations by HETE-2 of four short bursts: GRBs 010326b, 040802, 051211, and 060121. The durations and absence of spectral lags for the four bursts provides strong evidence that all four bursts are SPBs.

Of the four short bursts, GRB 060121 is the most fascinating. It is one of only a few short GRBs for which strong spectral evolution has been demonstrated. It is also the first short GRB for which it has been possible to obtain a photometric redshift from the optical and NIR afterglow of the burst. The result provides strong evidence that GRB 060121 lies at



a redshift  $z > 1.5$ , and more likely at a redshift  $z = 4.6$ , making this the first short burst for which a high redshift has been securely determined. The properties of GRB 060121, when taken together, provide very strong, but not conclusive, evidence that it is an SPB. If GRB 060121 is due to the merger of a compact binary, its high redshift and probable origin in a star-forming disk galaxy argue for a progenitor population that is diverse in terms of merger times and locations.

### **Acknowledgments**

The HETE-2 mission is supported in the US by NASA contract NASW-4690; in Japan, in part by the Ministry of Education, Culture, Sports, Science, and Technology Grant-in-Aid 13440063; and in France, by CNES contract 793-01-8479. KH is grateful for HETE-2 support under Contract MIT-SC-R-293291, for Mars Odyssey Support under NASA grant FDNAG5-11451.

## REFERENCES

- Aloy, M. A., Janka, H.-Th., & Mueller, E. 2005, *A&A*, 436, 273
- Amati, L. et al. 2002, *A&A*, 390, 81
- Arimoto, M. et al. 2006, *GCN Circ.* 4550
- Arnaud, K. A., 1996, *Astronomical Data Analysis Software and Systems V*, Eds. Jacoby G and Barnes J., p. 17, *ASP Conf. Series Volume 101*.
- Atteia, J-L, et al. 2003, in *Gamma-Ray Burst and Afterglow Astronomy 2001*, *AIP Conf. Proceedings 662*, ed. G. R. Ricker & R. K. Vanderspek (New York: AIP), 17
- Atteia, J.-L. et al. 2005, *GCN Circ.* 4324
- Balastegui, A., Ruiz-Laurent, P. & Canal, R. 2001, *MNRAS* 238, 283
- Band, D. et al. 1993, *ApJ*, 413, 281
- Barbier, L. et al. 2005, *GCN Circ.* 4194
- Barthelmy, S. et al. 2005a, *Nature*, 438, 994
- Barthelmy, S. et al. 2005b, *GCN Circ.* 3385
- Barthelmy, S. et al. 2005c, *GCN Circ.* 4401
- Barthelmy, S. et al. 2006, *GCN Circ.* 4879
- Belczynski, K. et al. 2006, *ApJ*, in press
- Berger, E., et al. 2005a, *Nature*, 438, 988
- Berger, E., 2005b, in *proc. of Swift GRB Symposium*
- Berger, E. & Soderberg, A. M. 2005, *GCN Circ.* 4384
- Bloom, J. S. et al. 2006, *ApJ*, 638, 354
- Boer, M. et al. 2006, *GCN Circ.* 4552
- Breeveld, A. A. et al. 2006, *GCN Circ.* 4567
- Bulik, T. Belczyński, K., & Zbijewski, W. 1999, *A&A Suppl.* 138, 483
- Castander, F. & Lamb, D. Q. 1999, *ApJ*, 523, 593

- Connaughton, V. 2002, *ApJ*, 567, 1028
- Costa, E., et al. 1997, *Nature* 387, 783-784
- Covino, S., et al. 2006, *A&A*, 447, L5
- Crew, G., et al. 2003, *ApJ*, 599, 387
- Cummings, J. et al. 2005a, *GCN Circ.* 4190
- Cummings, J. et al. 2005b, *GCN Circ.* 4365
- Donaghy, T. Q., Graziani, C., Lamb, D. Q., & Norris, J. P. 2006, in preparation
- Eichler, D., Livio, M., Piran, T., & Schramm, D. N. 1989, *Nature* 340, 126
- Fenimore, E. E., et al. 2004, *GCN Circ.* 2735
- Fox, D. B. & Moon, D.-S. 2004, *GCN Circ.* 2734
- Fox, D. B., et al. 2005, *Nature*, 437, 845
- Frederiks, D. D., et al. 2004, in *Gamma-Ray Bursts in the Afterglow Era*, ed. M. Feroci, F. Frontera, N. Masetti, and L. Piro (ASP, San Francisco) 197
- Fruchter, A., et al. 2002, *GCN Circ.* 1781
- Fruchter, A., et al. 2006, *Nature*, in press, (astro-ph/0603537)
- Fryer, C. L., Woosley, S. E. & Hartmann, D. H. 1999, 526, 152
- Gal-Yam, A., et al. 2006, *ApJ*, in press (astro-ph/0509891)
- Gehrels, N., et al. 2005, *Nature*, 437, 851
- Ghirlanda, G., et al. 2004, *A&A*, 422, L55
- Golenetskii, S. et al. 2005, *GCN Circ.* 4394
- Golenetskii, S. et al. 2006a, *GCN Circ.* 4564
- Golenetskii, S. et al. 2006b, *GCN Circ.* 4881
- Gorosabel, J. et al. 2006, *A&A*, 450, 87
- Guidorzi C. et al. 2005, *GCN Circ.* 4356

- Halpern, J. P. et al. 2005, GCN Circ. 4623
- Hearty, F. et al. 2006a, GCN Circ. 4604
- Hearty, F. et al. 2006b, GCN Circ. 4611
- Hjorth, J. et al. 2003, Nature, 423, 847
- Hjorth, J., et al. 2005, Nature, 437, 859
- Horváth, I. 1998, ApJ, 508, 757
- Horváth, I. 2002, A&A, 392, 791
- Horváth, I., et al. 2006, A&A, 447, 23
- Hullinger, D. et al. 2005, GCN Circ. 4400
- Hullinger, D. et al. 2006, GCN Circ. 5142
- Hurley, K. 1992, in Gamma-Ray Bursts, ed. W. Paciesas & G. Fishman (AIP, New York) 3
- Hurley, K. et al. 2004, GCN Circ. 2637
- Hurley, K., et al. 2005, Nature, 434, 1098
- Kawai, N., et al. 2003, in Gamma-Ray Burst and Afterglow Astronomy 2001, AIP Conf. Proceedings 662, ed. G. R. Ricker & R. K. Vanderspek (New York: AIP), 25
- Kawai, N. et al. 2005, GCN Circ. 4359
- Kouveliotou, C., et al. 1993, ApJ, 413, L101
- Krimm, H. et al. 2005, GCN Circ. 3667
- Krimm, H., et al. 2006, ApJ, submitted
- Lamb, D. Q., Graziani, C. & Smith, I. 1993, ApJ, 413, L11
- Lamb, D. Q., Donaghy, T. Q., & Graziani, C. 2005, ApJ, 520, 335
- Lamb, D. Q., et al. 2004, in Gamma-Ray Bursts in the Afterglow Era, ed. M. Feroci, F. Frontera, N. Masetti, and L. Piro (ASP, San Francisco) 94
- Lamb, D. Q., et al. 2006, ApJ, submitted (astro-ph/0206151)
- Lazzati, D., Ramirez-Ruiz, E. & Ghisellini, G. 2001, A&A 379, L39

- Levan, A. J. et al. 2006a, GCN Circ. 4562
- Levan, A. J., et al. 2006b, ApJ, submitted (astro-ph/0603282)
- Liang, E. W., Dai, Z. G. & Wu, X. F. 2004, ApJ, 606, L29
- Malesani, D. et al. 2006, GCN Circ. 4561
- Mangano, V. et al. 2006a, GCN Circ. 4560
- Mangano, V. et al. 2006b, GCN Circ. 4565
- Markwardt, C. et al. 2006, GCN Circ. 4873
- Mazets, E. P. & Golenetskii, S. V. 1981, Ap&SS, 75, 47
- Metzger, M R. et al. 1997, Nature 387, 878
- Nakar, E., Gal-Yam, & Fox, D. B. 2006, ApJ, submitted (astro-ph/0511254)
- Narayan, R., Paczyński, B., & Piran, T. 1992, ApJ, 395, L83
- Norris, J. P., Nemiroff, R. J. & Davis, S. P. 1994, in AIP Conf. Proc. 307, Gamma-Ray Bursts, ed. G. J. Fishman, J. J. Brainerd, & K. Hurley (New York: AIP), 172
- Norris, J. P., et al. 1996, ApJ, 459, 393
- Norris, J. P. 2002, ApJ, 579, 386
- Norris, J. P. & Bonnell, J. T. 2006, ApJ, in press (astro-ph/0601190)
- Norris, J. P. et al. 2005a, GCN Circ. 4377
- Norris, J. P. et al. 2005b, GCN Circ. 4388
- Oechslin, R., & Janka, H.-Th. 2006, A&A, submitted (astro-ph/0507099)
- Ofek, E. O. et al. 2006, GCN Circ. 5123
- Palmer, D. M., et al. 2005, Nature, 434, 1107
- Parsons, A. et al. 2005, GCN Circ. 3935
- van Paradijs, J. et al. 1997, Nature, 386, 686
- Lee, T. T., & Petrosian, V. 1996, ApJ, 470, 479

- Postigo, A., et al. 2006, *Nature*, submitted
- Price, P. et al. 2001, *GCN Circ.* 1020
- Prigozhin, G. et al. 2006, *GCN Circ.* 4551
- Prochaska, J. X. et al. 2006, *ApJ*, 642, 989
- Reichart, D. E., et al. 2001, *ApJ*, 552, 57
- Ricker, G.R. et al. 2003, in *Gamma-Ray Burst and Afterglow Astronomy 2001*, AIP Conf. Proceedings 662, ed. G. R. Ricker & R. K. Vanderspek (New York: AIP), 3
- Ricker, G. R. et al. 2001, *GCN Circ.* 1018
- Rosswog, S., Ramirez-Ruiz, E., & Davies, M. B. 2003, *MNRAS*, 345, 1077
- Sakamoto, T. et al. 2005a, *ApJ*, 629, 311
- Sakamoto, T. et al. 2005b, *GCN Circ.* 3010
- Sakamoto, T. et al. 2005c, *GCN Circ.* 4403
- Sakamoto, T. et al. 2006, in *proc. Swift GRB Symposium*
- Sato, G. et al. 2005a, *GCN Circ.* 3793
- Sato, G. et al. 2005b, *GCN Circ.* 4318
- Sato, G. et al. 2006, *GCN Circ.* 5064
- Schady, P. et al. 2006, *GCN Circ.* 4877
- Soderberg, A. M., et al. 2006, *ApJ*, submitted (astro-ph/0601455)
- Stanek, C., et al. 2003, *ApJ*, 591, L17
- Thorne, K. S., & Cutler, C. 2002, *General Relativity and Gravitation*, ed. N. Bishop & S. D. Maharaj (Singapore: World Scientific), 72
- Villasenor, J.N., et al. 2003, in *Gamma-Ray Burst and Afterglow Astronomy 2001*, AIP Conf. Proceedings 662, ed. G. R. Ricker & R. K. Vanderspek (New York: AIP), 33
- Villasenor, J., et al. 2005, *Nature*, 437, 855
- Vreeswijk, P., et al. 2002, *GCN Circ.* 1785

Wiersema, K., et al. 2004, GCN Circ. 2800

Woosley, S. E. 1993, ApJ, 405, 2731

Yonetoku, D., et al. 2004, ApJ, 609, 935

Zhang, W., Woosley, S. E., & MacFadyen, A. I. 2003, ApJ, 586, 356

Table 1. Localization Histories for Four HETE-2 short GRBs.

Source	Time (UTC)	$\alpha$	$\delta$	Radius	Offset
GRB 010326B					
HETE Trigger 1496	08:33:12	—	—	—	—
WXM Ground	13:18:18	11 24 23.36	-11 09 57	21'	—
GRB 040802					
HETE Trigger 3485	18:02:21.03	—	—	—	—
WXM Last	18:08:07	19 26 57	19 25 11	30'	—
WXM Ground	11:30:53	18 36 48	-48 36 19	540' $\times$ 16'	—
WXM Ground Rev	17:18:58	18 47 24	-44 29 20	600' $\times$ 16'	—
IPN Intersection	21:45:12	18 52 30	-42 39 32	20' $\times$ 5'	—
GRB 051211					
HETE Trigger 3979	02:50:05.36	—	—	—	—
WXM Flight	02:52:22	06 49 48	26 35 57	30'	—
SXC Ground	05:58:30	06 56 13	32 40 44	1.3'	—
GRB 060121					
HETE Trigger 4010	22:24:54.49	—	—	—	—
WXM Flight	22:28:24	09 09 22	45 45 59	14'	8.13'
WXM Ground	23:12:35	09 10 04	45 41 24	8'	2.67'
SXC Ground	23:53:06	09 09 57	45 40 30	80''	1.16'
X-Ray Transient	01:21:37	09 09 52.13	45 39 44.9	3.7''	2.15''
Optical Transient	—	09 09 51.93	45 39 45.4	0.5''	—

Note. — Ra ( $\alpha$ ) is given in hours, minutes and seconds, while Dec ( $\delta$ ) is given in degrees, arcminutes and arcseconds, for the J2000 epoch. The position error radius is for 90% confidence. The offsets given for 060121 are from the optical transient.



Table 2. Temporal Properties of Four HETE-2 short GRBs.

Energy (keV)	$T_{50}$ (s)	$T_{90}$ (s)	Energy (keV)	$T_{50}$ (s)	$T_{90}$ (s)
GRB 010326B			GRB 040802		
WXM			WXM		
2–10	$1.85 \pm 0.41$	$5.44 \pm 1.70$	2–10	–	–
10–25	$1.54 \pm 0.96$	$4.69 \pm 2.73$	10–25	–	–
Fregate			Fregate		
6–15	$1.03 \pm 0.12$	$3.10 \pm 0.94$	6–15	$1.45 \pm 0.25$	$3.44 \pm 0.76$
15–30	$1.16 \pm 0.13$	$2.54 \pm 0.27$	15–30	$1.31 \pm 0.10$	$2.45 \pm 0.18$
6–40	$1.10 \pm 0.10$	$3.22 \pm 0.67$	6–40	$1.38 \pm 0.14$	$3.01 \pm 0.22$
30–85	$0.69 \pm 0.17$	$2.05 \pm 0.47$	30–85	$1.01 \pm 0.08$	$2.50 \pm 0.16$
30–400	$0.70 \pm 0.15$	$1.90 \pm 0.48$	30–400	$0.85 \pm 0.05$	$2.31 \pm 0.16$
85–400	$0.88 \pm 0.18$	$2.05 \pm 0.65$	85–400	$0.54 \pm 0.05$	$1.35 \pm 0.34$
GRB 051211			GRB 060121		
WXM			WXM		
2–10	–	–	2–10	$3.92 \pm 0.73$	$10.93 \pm 2.18$
10–25	–	–	10–25	$2.14 \pm 0.35$	$11.58 \pm 1.60$
Fregate			Fregate		
6–15	–	–	6–15	$1.23 \pm 0.10$	$3.14 \pm 0.25$
15–30	–	–	15–30	$1.16 \pm 0.05$	$2.91 \pm 0.16$
6–40	$2.19 \pm 0.81$	$4.82 \pm 0.79$	6–40	$1.10 \pm 0.10$	$2.40 \pm 0.16$
30–85	$2.71 \pm 0.48$	$6.72 \pm 1.51$	30–85	$0.91 \pm 0.03$	$2.21 \pm 0.10$
30–400	$1.83 \pm 0.16$	$4.25 \pm 0.56$	30–400	$0.88 \pm 0.03$	$1.97 \pm 0.06$
85–400	$1.60 \pm 0.21$	$4.02 \pm 1.28$	85–400	$0.70 \pm 0.04$	$1.60 \pm 0.07$

Note. — Errors are  $1\text{-}\sigma$ . If a band has no duration listed that indicates that the signal in that band was not strong enough to obtain a reliable duration.

Table 3. Durations and Spectral Lags for Some HETE-2 Short GRBs

GRB	$T_{90}$ [sec]	Band [keV]	Lag [ms]	Error [ms]	Binning [ms]
010326B	$1.62 \pm 0.28$	40-80 vs. 80-400	-4	+24 -32	64
		6-40 vs. 80-400	-2	+16 -20	
020531	$1.02 \pm 0.15$	40-80 vs. 80-400	-20	+32 -22	64
		6-40 vs. 80-400	14	+10 -20	
021211	$2.67 \pm 0.24$	40-80 vs. 80-400	116	+36 -38	64
		6-40 vs. 80-400	140	+18 -24	
040802	$2.32 \pm 0.23$	40-80 vs. 80-400	29	+32 -30	32
		6-40 vs. 80-400	-6	+15 -16	
040924	$2.39 \pm 0.24$	40-80 vs. 80-400	42	+7 -11	8
		6-40 vs. 80-400	37	+9 -6	
050709	$0.07 \pm 0.01$	40-80 vs. 80-400	-4.0	+2.5 -2.5	4
		6-40 vs. 80-400	1.8	+2.6 -2.6	
051211	$4.25 \pm 0.56$	40-80 vs. 80-400	-2	+23 -23	16
		6-40 vs. 80-400	–	– –	
060121	$1.97 \pm 0.06$	40-80 vs. 80-400	2	+29 -14	8
		6-40 vs. 80-400	17	+9 -9	

Note. — Spectral lags for some HETE-2 GRBs whose durations indicated they were possibly short GRBs. All durations are for the 30-400 keV Fregate band.

Table 4. Spectral Model Parameters for GRBs 010326B, 040802 and 051211.

Time	Model	$\alpha$	$\beta$	$E_{\text{peak}}^{\text{obs}}$ [keV]	Norm (at 15 keV) [ph cm <sup>-2</sup> s <sup>-1</sup> keV <sup>-1</sup> ]	$\chi^2/\text{d.o.f}$
GRB 010326B						
-1.3–2.2	PL	$-1.62^{+0.07}_{-0.07}$	—	—	$0.082^{+0.009}_{-0.008}$	120.2/112
	PLE	$-1.08^{+0.25}_{-0.22}$	—	$51.8^{+18.6}_{-11.3}$	$0.132^{+0.031}_{-0.023}$	95.0/111
	Band	$-1.08^{+0.22}_{-0.19}$	-9.33	$51.7^{+12.6}_{-11.0}$	$0.132^{+0.017}_{-0.019}$	95.0/110
GRB 040802						
-1.0–4.0	PL	$-1.60^{+0.06}_{-0.06}$	—	—	$0.171^{+0.016}_{-0.015}$	173.5/125
	PLE	$-0.85^{+0.23}_{-0.20}$	—	$92.2^{+18.8}_{-13}$	$0.176^{+0.021}_{-0.020}$	118.0/124
	Band	$-0.86^{+0.16}_{-0.19}$	-9.30	$93.7^{+17.3}_{-14.6}$	$0.175^{+0.019}_{-0.022}$	118.0/123
GRB 051211						
-0.5–2.7	PL	$-1.25^{+0.09}_{-0.09}$	—	—	$0.058^{+0.011}_{-0.010}$	140.6/137
	PLE	$-0.07^{+0.50}_{-0.41}$	—	$121^{+33.0}_{-20.3}$	$0.045^{+0.013}_{-0.013}$	103.5/136
	Band	$-0.12^{+0.54}_{-0.21}$	-9.36	$125^{+29.3}_{-24.1}$	$0.046^{+0.013}_{-0.013}$	103.5/135

Note. — Errors are for 90% confidence.

Table 5. Spectral Model Parameters for GRB 060121.

Time	Model	$\alpha$	$\beta$	$E_{\text{peak}}^{\text{obs}}$ [keV]	Norm (at 15 keV) [ph cm <sup>-2</sup> s <sup>-1</sup> keV <sup>-1</sup> ]	$\chi^2/\text{d.o.f}$
0.0–1.75	PL	$-1.87^{+0.14}_{-0.15}$	—	—	$0.109 \pm 0.018$	128.5/135
	PLE	$-1.03^{+0.47}_{-0.43}$	—	$56.0^{+21.2}_{-12.5}$	$0.140^{+0.033}_{-0.029}$	114.3/134
	Band	$-1.09^{+0.54}_{-0.37}$	-9.30	$57.4^{+19.7}_{-14.0}$	$0.138^{+0.036}_{-0.026}$	114.2/133
1.75–2.7	PL	-1.27	—	—	0.506	335.6/135
	PLE	$-0.41^{+0.13}_{-0.12}$	—	$137^{+14.7}_{-12.0}$	$0.487^{+0.037}_{-0.036}$	121.6/134
	Band	$-0.42^{+0.10}_{-0.11}$	-8.18	$138^{+13.9}_{-12.8}$	$0.486^{+0.037}_{-0.035}$	121.6/133
2.7–3.64	PL	-1.56	—	—	0.458	520.7/135
	PLE	$-0.20^{+0.17}_{-0.16}$	—	$84.6^{+6.3}_{-5.7}$	$0.521^{+0.045}_{-0.044}$	175.4/134
	Band	$-0.23^{+0.21}_{-0.13}$	-9.37	$87.0^{+3.8}_{-8.2}$	$0.513^{+0.054}_{-0.036}$	175.9/133
3.64–5.186	PL	$-1.99^{+0.13}_{-0.12}$	—	—	$0.123 \pm 0.019$	256.7/135
	PLE	$-0.86^{+0.35}_{-0.32}$	—	$43.6^{+9.9}_{-8.0}$	$0.202^{+0.053}_{-0.040}$	211.3/134
	Band	$-0.89^{+0.19}_{-0.30}$	-9.37	$44.6^{+8.8}_{-9.1}$	$0.197^{+0.058}_{-0.035}$	211.4/133
5.186–10.0	PL	$-2.52^{+0.41}_{-0.54}$	—	—	$0.030 \pm 0.010$	98.2/135
	PLE	$-1.51^{+1.22}_{-8.49}$	—	$8.5^{+10.1}_{-8.5}$	$0.086^{+0.410}_{-0.051}$	94.8/134
	Band	$-1.93^{+0.20}_{-8.07}$	-9.27	$3.1^{+18.4}_{-3.1}$	$0.044^{+0.134}_{-0.011}$	96.0/133
1.75–3.64	PL	-1.32	—	—	0.484	499.1/135
	PLE	$-0.41 \pm 0.10$	—	$118^{+8.9}_{-7.6}$	$0.493 \pm 0.027$	125.1/134
	Band	$-0.32^{+0.13}_{-0.11}$	$-2.52^{+0.26}_{-0.52}$	$108^{+9.6}_{-8.9}$	$0.501^{+0.030}_{-0.028}$	118.3/133
0.0–3.64	PL	-1.38	—	—	0.313	429.9/135
	PLE	$-0.50^{+0.11}_{-0.10}$	—	$112^{+8.9}_{-7.6}$	$0.320 \pm 0.018$	123.5/134
	Band	$-0.46^{+0.13}_{-0.12}$	$-2.72^{+0.36}_{-1.87}$	$107^{+10.7}_{-8.9}$	$0.323 \pm 0.019$	120.5/133
0.0–5.186	PL	-1.42	—	—	0.263	406.1/135
	PLE	$-0.60 \pm 0.10$	—	$108^{+8.9}_{-7.4}$	$0.275 \pm 0.015$	115.6/138
	Band	$-0.58^{+0.12}_{-0.10}$	$-3.12^{+0.64}_{-6.88}$	$106^{+9.4}_{-9.1}$	$0.276^{+0.016}_{-0.015}$	114.7/133
0.0–10.0	PL	$-1.45 \pm 0.03$	—	—	$0.155 \pm 0.008$	251.4/135
	PLE	$-0.79^{+0.12}_{-0.11}$	—	$114^{+14.2}_{-10.9}$	$0.162 \pm 0.010$	111.8/134
	Band	$-0.78^{+0.12}_{-0.11}$	$-2.99^{+0.70}_{-7.01}$	$112^{+14.2}_{-12.3}$	$0.162^{+0.011}_{-0.010}$	111.2/133
71.2–121.6	PL	$-2.81^{+1.14}_{-2.11}$	—	—	—	22.9/20

Note. — Errors are for 90% confidence. Some PL fit parameters are quoted without errorbars because XSPEC fails to compute an error region when the  $\chi^2$  per d.o.f. is greater than 2. Some Band model  $\beta$  values are quoted without errorbars because in those cases, the minimum and maximum  $\beta$  were found to be the minimum and maximum parameter bounds; i.e. the parameter was unconstrained by the data.

Table 6. Burst-Average Emission Properties of Four HETE-2 Short GRBs.

Energy (keV)	Peak Photon Flux (ph cm <sup>-2</sup> s <sup>-1</sup> )	Photon Fluence (ph cm <sup>-2</sup> )	Peak Energy Flux (10 <sup>-8</sup> erg cm <sup>-2</sup> s <sup>-1</sup> )	Energy Fluence (10 <sup>-8</sup> erg cm <sup>-2</sup> )
GRB 010326B				
2–10	2.79 ± 1.09	11.9 ± 4.0	2.34 ± 0.81	8.98 ± 2.61
2–25	4.78 ± 1.34	16.5 ± 4.4	7.57 ± 1.49	21.0 ± 3.7
2–30	5.17 ± 1.35	17.2 ± 4.4	9.25 ± 1.62	24.2 ± 3.9
7–30	3.10 ± 0.53	7.71 ± 1.1	7.92 ± 1.19	18.3 ± 2.34
30–400	1.92 ± 0.29	3.24 ± 0.53	18.9 ± 4.0	33.1 ± 8.4
50–100	0.76 ± 0.14	1.21 ± 0.23	8.33 ± 1.55	13.3 ± 2.6
100–300	0.22 ± 0.10	0.42 ± 0.22	4.78 ± 2.38	9.67 ± 5.50
2–400	7.05 ± 1.36	20.5 ± 4.4	28.1 ± 4.3	57.1 ± 9.5
GRB 040802				
2–10	6.77 ± 2.20	17.2 ± 5.4	5.45 ± 1.58	13.8 ± 3.9
2–25	10.8 ± 2.69	27.1 ± 6.4	16.0 ± 2.8	39.7 ± 6.5
2–30	11.6 ± 2.73	29.0 ± 6.5	19.5 ± 3.0	47.9 ± 6.8
7–30	6.38 ± 0.93	15.7 ± 2.05	16.1 ± 2.0	39.4 ± 4.4
30–400	6.44 ± 0.51	12.3 ± 0.89	93.9 ± 11.6	152 ± 18
50–100	2.37 ± 0.22	4.76 ± 0.40	26.9 ± 2.5	53.5 ± 4.5
100–300	1.83 ± 0.27	2.63 ± 0.48	46.8 ± 8.0	64.0 ± 13.8
2–400	18.0 ± 2.74	41.1 ± 6.5	113 ± 12	200 ± 20
GRB 051211				
2–10	0.90 ± 0.71	1.35 ± 0.84	0.78 ± 0.57	1.21 ± 0.70
2–25	1.77 ± 1.01	2.98 ± 1.33	3.13 ± 1.35	5.71 ± 1.97
2–30	1.98 ± 1.04	3.43 ± 1.39	4.07 ± 1.49	7.65 ± 2.28
7–30	1.34 ± 0.51	2.51 ± 0.78	3.66 ± 1.18	7.04 ± 1.90
30–400	1.55 ± 0.28	4.99 ± 0.52	17.1 ± 3.83	72.4 ± 12.2
50–100	0.67 ± 0.14	1.89 ± 0.12	7.46 ± 1.59	23.0 ± 2.9
100–300	0.25 ± 0.11	1.50 ± 0.33	5.75 ± 2.81	37.2 ± 9.7
2–400	3.48 ± 1.04	8.37 ± 1.57	21.1 ± 4.2	80.0 ± 12.9

Table 6—Continued

Energy (keV)	Peak Photon Flux (ph cm <sup>-2</sup> s <sup>-1</sup> )	Photon Fluence (ph cm <sup>-2</sup> )	Peak Energy Flux (10 <sup>-8</sup> erg cm <sup>-2</sup> s <sup>-1</sup> )	Energy Fluence (10 <sup>-8</sup> erg cm <sup>-2</sup> )
GRB 060121				
2–10	5.62 ± 1.05	29.0 ± 4.9	4.96 ± 0.83	23.8 ± 3.6
2–25	11.4 ± 1.4	47.9 ± 5.9	20.4 ± 1.9	73.5 ± 6.3
2–30	12.7 ± 1.5	51.6 ± 6.0	26.3 ± 2.1	89.8 ± 6.7
7–30	8.75 ± 0.70	29.6 ± 2.1	23.7 ± 1.6	75.5 ± 4.5
30–400	14.1 ± 0.6	28.5 ± 1.2	211 ± 14	387 ± 27
50–100	5.39 ± 0.28	10.9 ± 0.5	61.7 ± 3.2	123 ± 6.
100–300	4.39 ± 0.34	7.32 ± 0.67	111 ± 10	182 ± 20
2–400	26.8 ± 1.6	80.2 ± 6.1	237 ± 14	477 ± 28

Note. — All of the quantities in this table are derived assuming a cutoff powerlaw for the spectrum. Errors are for 90% confidence.

Table 7. Time Resolved Fluences for GRB 060121.

Energy	0.0-1.75	1.75-2.7	2.7-3.64	3.64-5.186	5.186-10.0
	Energy Fluence [ $10^{-8}$ erg $\text{cm}^{-2}$ ]				
2–10	$4.80 \pm 2.22$	$4.76 \pm 0.81$	$3.92 \pm 0.78$	$4.69 \pm 1.55$	$20.0 \pm 12.0$
2–25	$11.3 \pm 3.0$	$19.5 \pm 1.8$	$17.4 \pm 1.8$	$12.0 \pm 2.3$	$24.2 \pm 12.6$
2–30	$13.0 \pm 3.1$	$25.3 \pm 2.0$	$22.8 \pm 2.0$	$13.9 \pm 2.4$	$24.8 \pm 12.6$
7–30	$9.87 \pm 1.71$	$22.7 \pm 1.6$	$20.7 \pm 1.6$	$11.0 \pm 1.6$	$7.99 \pm 2.68$
30–400	$19.7 \pm 5.2$	$207 \pm 14$	$105 \pm 8$	$16.2 \pm 4.0$	$6.49 \pm 4.63$
50–100	$7.98 \pm 1.92$	$59.5 \pm 3.2$	$43.1 \pm 2.7$	$7.04 \pm 1.73$	$1.89 \pm 1.29$
100–300	$6.14 \pm 3.29$	$110 \pm 10$	$39.5 \pm 5.9$	$3.23 \pm 1.88$	$2.19 \pm 2.19$
2–400	$32.6 \pm 6.0$	$232 \pm 14$	$128 \pm 8$	$30.0 \pm 4.7$	$28.9 \pm 11.3$
	Photon Number Fluence [ $\text{ph cm}^{-2}$ ]				
2–10	$6.41 \pm 3.35$	$5.40 \pm 1.02$	$4.33 \pm 0.96$	$6.00 \pm 2.26$	$36.4 \pm 23.6$
2–25	$8.91 \pm 3.67$	$10.9 \pm 1.4$	$9.30 \pm 1.34$	$8.80 \pm 2.54$	$38.2 \pm 23.8$
2–30	$9.30 \pm 3.66$	$12.2 \pm 1.4$	$10.6 \pm 1.4$	$9.26 \pm 2.54$	$38.3 \pm 23.8$
7–30	$4.12 \pm 0.83$	$8.37 \pm 0.68$	$7.58 \pm 0.68$	$4.54 \pm 0.73$	$4.09 \pm 1.42$
30–400	$1.90 \pm 0.38$	$13.7 \pm 0.6$	$9.08 \pm 0.49$	$1.78 \pm 0.34$	$0.55 \pm 0.34$
50–100	$0.72 \pm 0.17$	$5.20 \pm 0.28$	$3.84 \pm 0.24$	$0.65 \pm 0.15$	$0.17 \pm 0.12$
100–300	$0.26 \pm 0.13$	$4.33 \pm 0.34$	$1.73 \pm 0.23$	$0.15 \pm 0.08$	$0.08 \pm 0.08$
2–400	$11.3 \pm 3.7$	$25.9 \pm 1.5$	$19.6 \pm 1.4$	$11.0 \pm 2.5$	$38.7 \pm 23.6$



Table 8. Well-Localized Short GRBs.

GRB	Loc	XA	OA	z	Host <sup>a</sup>	$T_{90}^b$ [sec]	P(S  $T_{90}$ )	Lag <sup>c</sup> [ms]	Spectral Fit		Refs <sup>d</sup>
									$\alpha$	$E_{\text{peak}}^{\text{obs}}$	
<b>010326B</b>	HETE	–	–	–	–	$1.62 \pm 0.28$	0.972	$-4_{-32}^{+24}$	$-1.08_{-0.22}^{+0.25}$	$51.8_{-11.3}^{+18.6}$	–,–,1,1,3
020531	H/I	–	–	–	–	$1.02 \pm 0.15$	0.995	$-20_{-22}^{+32}$	$-0.83_{-0.13}^{+0.14}$	$231_{-58.11}^{+113.1}$	–,–,4,1,4
021211 <sup>e</sup>	HETE	Y	Y	1.01	S	$2.67 \pm 0.24$	0.866	$116_{-38}^{+36}$	$-0.86_{-0.09}^{+0.10}$	$45.6_{-6.2}^{+7.8}$	5,6,1,1,3
<b>040802</b>	H/I	–	–	–	–	$2.32 \pm 0.23$	0.911	$29_{-30}^{+32}$	$-0.85_{-0.20}^{+0.23}$	$92.2_{-13}^{+18.8}$	–,–,1,1,1
040924	HETE	Y	Y	0.859	S	$2.39 \pm 0.24$	0.902	$42_{-11}^{+7}$	$-1.03_{-0.08}^{+0.09}$	$41.9_{-5.3}^{+6.5}$	7,8,1,1,1
050202	Swift	–	–	–	–	0.08	1.000	–	$-1.4 \pm 0.3$	–	–,–,9,–,9
050509B	Swift	Y	–	0.225?	E?	$0.040 \pm 0.004$	1.000	$4.3_{-3.0}^{+3.2}$	$-1.5 \pm 0.4$	–	10,11,11,2,12
050709	HETE	Y	Y	0.1606	S	$0.07 \pm 0.01$	1.000	$-4.0 \pm 2.5$	$-0.53_{-0.13}^{+0.12}$	$83.9_{-8.3}^{+11}$	13,13,14,1,14
050724	Swift	Y	Y	0.258	E	$3.0 \pm 1.0$	0.816	$-4.2_{-6.6}^{+8.2}$	$-1.71 \pm 0.16$	–	15,16,17,2,18
050813	Swift	Y	–	1.8?	?	$0.6 \pm 0.1$	0.999	$-9.7_{-11.0}^{+14.0}$	$-1.19 \pm 0.33$	–	19,19,20,2,20
050906	Swift	–	–	–	–	$0.128 \pm 0.016$	1.000	–	$-1.91 \pm 0.42$	–	–,–,21,–,21
051105A	Swift	–	–	–	–	$0.028 \pm 0.004$	1.000	$6.3_{-4.8}^{+5.3}$	$-1.33 \pm 0.35$	–	–,–,22,2,23
051210	Swift	Y	–	–	–	$1.4 \pm 0.2$	0.983	$-5.3_{-22.0}^{+24.0}$	$-1.1 \pm 0.3$	–	–,–,24,2,24
<b>051211</b>	HETE	–	–	–	–	$4.25 \pm 0.56$	0.601	$-2 \pm 23$	$-0.07_{-0.41}^{+0.50}$	$121_{-20.3}^{+33.0}$	–,–,1,1,1
051221A	Swift	Y	Y	0.5465	S	$1.4 \pm 0.2$	0.983	$0.8 \pm 0.5$	$-1.08_{-0.14}^{+0.13}$	$402_{-72}^{+93}$	25,25,26,27,28
051227	Swift	Y	Y	–	–	$8.0 \pm 0.2$	0.200	$2 \pm 10$	$-0.40_{-1.06}^{+0.74}$	$100_{-41.3}^{+219}$	–,–,29,30,31
<b>060121</b>	HETE	Y	Y	1.5/4.6?	S?	$1.97 \pm 0.06$	0.946	$2_{-14}^{+29}$	$-0.79_{-0.11}^{+0.12}$	$114_{-10.9}^{+14.2}$	32,33,1,1,1
060313	Swift	Y	Y	< 1.7	–	$0.7 \pm 0.1$	0.999	$0.3 \pm 0.7$	$-0.60_{-0.22}^{+0.19}$	$922_{-177}^{+306}$	34,–,35,36,37
060502B	Swift	Y	–	–	–	$0.090 \pm 0.020$	1.000	$-0.2 \pm 2.8$	$-0.92 \pm 0.23$	–	–,–,38,38,38
060505	Swift	Y	Y	0.089?	S?	$4.0 \pm 1.0$	0.644	–	$-1.3 \pm 0.3$	–	39,39,40,–,40

Note. — See next page for explanations.

Note. – A summary of promptly localized short GRBs by HETE-2 and Swift; the bursts listed in bold face are the four detailed in this paper. H/I denotes bursts localized by HETE-2 where the size of the error box was greatly reduced by the IPN. <sup>a</sup>Morphology of the host galaxy, E=Elliptical, S=Star-Forming. <sup>b</sup> $T_{90}$  duration in the 30-400 keV band for HETE-2 bursts, and in the 15-350 keV band for Swift bursts. <sup>c</sup>Spectral lag between the 40-80 and 80-400 keV bands for HETE-2 bursts, and between the 25-50 and 100-350 keV bands for Swift bursts, except GRBs 050509B, 050724 and 051105A, which are between the 15-25 and 50-100 keV bands [see Norris & Bonnell (2006) for details]. <sup>d</sup>Citations for redshift, host galaxy,  $T_{90}$ , spectral lag and spectral fit. <sup>e</sup>The best fit for GRB 021211 is a Band model with the values quoted here for  $\alpha$  and  $E_{\text{peak}}^{\text{obs}}$ , and a high-energy powerlaw index  $\beta = -2.18_{-0.25}^{+0.14}$ . Citations: 1=this paper, 2=Norris & Bonnell (2006), 3=Sakamoto et al. (2005a), 4=Lamb et al. (2006), 5=Vreeswijk et al. (2002), 6=Fruchter et al. (2002), 7=Wiersema et al. (2004), 8=Fox & Moon (2004), 9=Sakamoto et al. (2005b), 10=Bloom et al. (2006), 11=Gehrels et al. (2005) 12=Barthelmy et al. (2005b), 13=Fox et al. (2005), 14=Villasenor et al. (2005), 15=Prochaska et al. (2006), 16=Berger et al. (2005a), 17=Barthelmy et al. (2005a), 18=Krimm et al. (2005), 19=Berger (2005b), 20=Sato et al. (2005a), 21=Parsons et al. (2005), 22=Cummings et al. (2005a), 23=Barbier et al. (2005), 24=Sato et al. (2005b), 25=Soderberg et al. (2006), 26=Cummings et al. (2005b), 27=Norris et al. (2005b), 28=Golenetskii et al. (2005), 29=Hullinger et al. (2005), 30=Barthelmy et al. (2005c), 31=Sakamoto et al. (2005c), 32=Postigo et al. (2006), 33=Levan et al. (2006b), 34=Schady et al. (2006), 35=Markwardt et al. (2006), 36=Barthelmy et al. (2006), 37=Golenetskii et al. (2006b), 38=Sato et al. (2006), 39=Ofek et al. (2006), 40=Hullinger et al. (2006).

Table 9. Short- Versus Long-Population Scorecard for HETE-2 and Swift Short GRBs

Criterion	$T_{90}$	Pulse Width	Spectral Hardness	Spectral Lag	Long, Soft Bump	$E_{\gamma}$	Location in Host Galaxy	Supernova Limit	Type of Host Galaxy
<i>Rating</i>	<i>Silver</i>	<i>Silver</i>	<i>Bronze</i>	<i>Gold</i>	<i>Gold</i>	<i>Silver</i>	<i>Gold</i>	<i>Gold</i>	<i>Gold</i>
010326B	Y	?	N	–	?	?	?	–	?
020531	Y	–	Y	Y	–	?	?	–	?
021211	–	N	N	N	–	?	N	–	–
040802	Y	–	–	–	?	?	?	–	?
040924	Y	N	N	N	–	?	–	N	–
050202	Y	Y	?	?	?	?	?	–	?
050509B	Y	Y	?	Y	–	Y	Y?	Y	Y?
050709	Y	Y	Y	Y	Y	Y	Y	Y	–
050724	–	–	?	Y	Y	Y	Y	–	Y
050813	Y	Y	?	Y	–	?	?	–	–
050906	Y	Y	?	?	?	?	?	–	?
051105A	Y	Y	?	Y	?	?	?	–	?
051210	Y	N	?	–	?	?	?	–	?
051211	–	N	Y	–	–	?	?	–	?
051221A	Y	–	Y	Y	–	Y	Y	Y	–
051227	–	N	Y	Y	Y	?	?	–	?

Table 9—Continued

Criterion	$T_{90}$	Pulse Width	Spectral Hardness	Spectral Lag	Long, Soft Bump	$E_\gamma$	Location in Host Galaxy	Supernova Limit	Type of Host Galaxy
<i>Rating</i>	<i>Silver</i>	<i>Silver</i>	<i>Bronze</i>	<i>Gold</i>	<i>Gold</i>	<i>Silver</i>	<i>Gold</i>	<i>Gold</i>	<i>Gold</i>
060121 (z=1.5)	Y	–	Y	–	Y	Y	Y?	–	–
(z=4.6)	Y	Y	Y	Y	Y	Y	Y?	–	–
060313	Y	?	Y	Y	–	?	?	–	?
060502B	Y	Y	?	Y	?	?	?	–	?
060505	–	N	?	?	?	?	?	Y?	?

Note. — Scorecard detailing nine criteria for a burst to belong to the short-population (not including detection of gravitational waves). For each well-localized short burst, we note whether it fits the criteria (Y) or not (N), or whether the data is inconclusive (–) or not available (?).

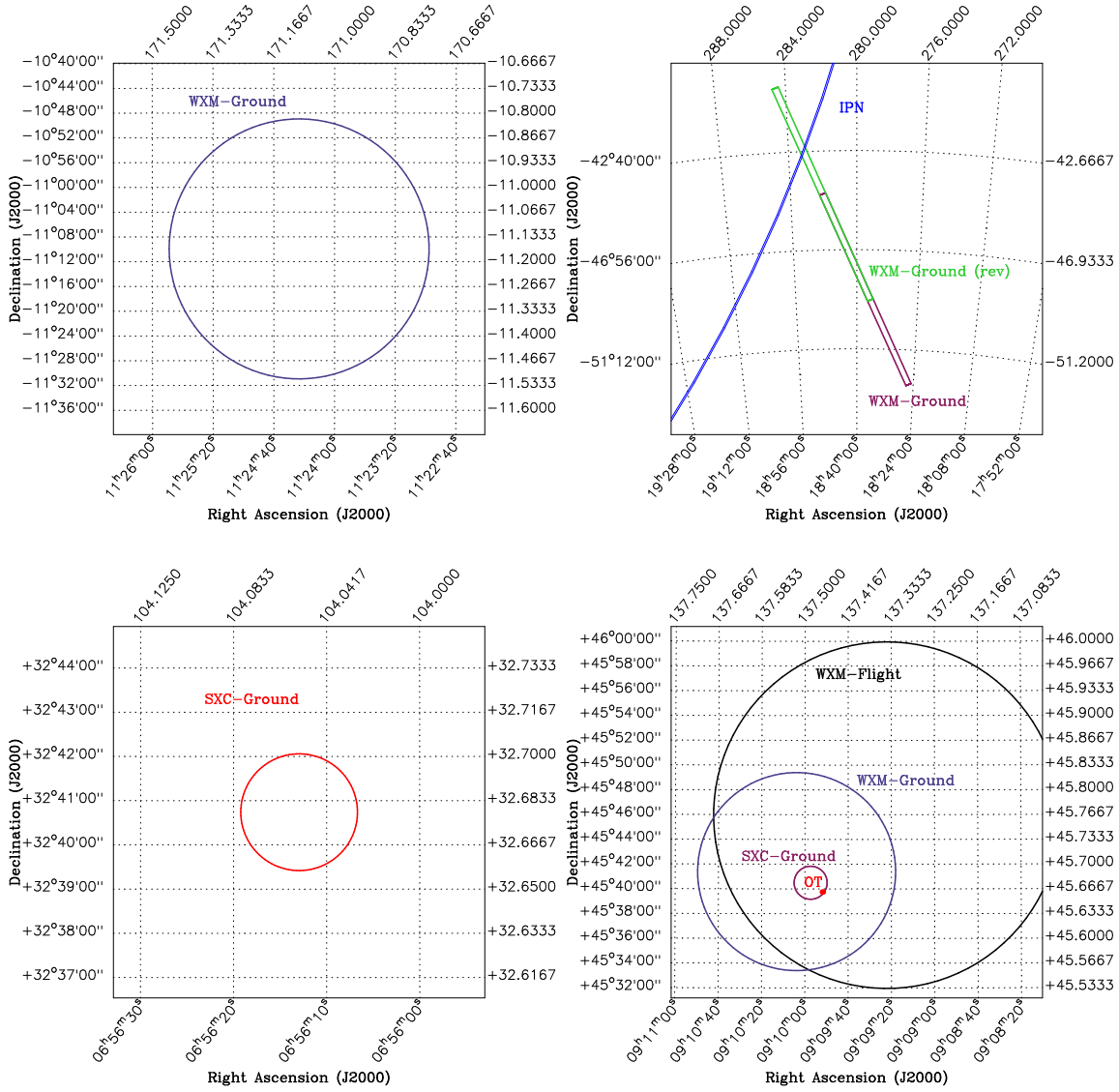


Fig. 1.— Skymaps summarizing the localizations of GRBs 010326B (upper left), 040802 (upper right), 051211 (lower left) and 060121 (lower right) as reported in the GCN Burst Position Notices; cf. Table 1.

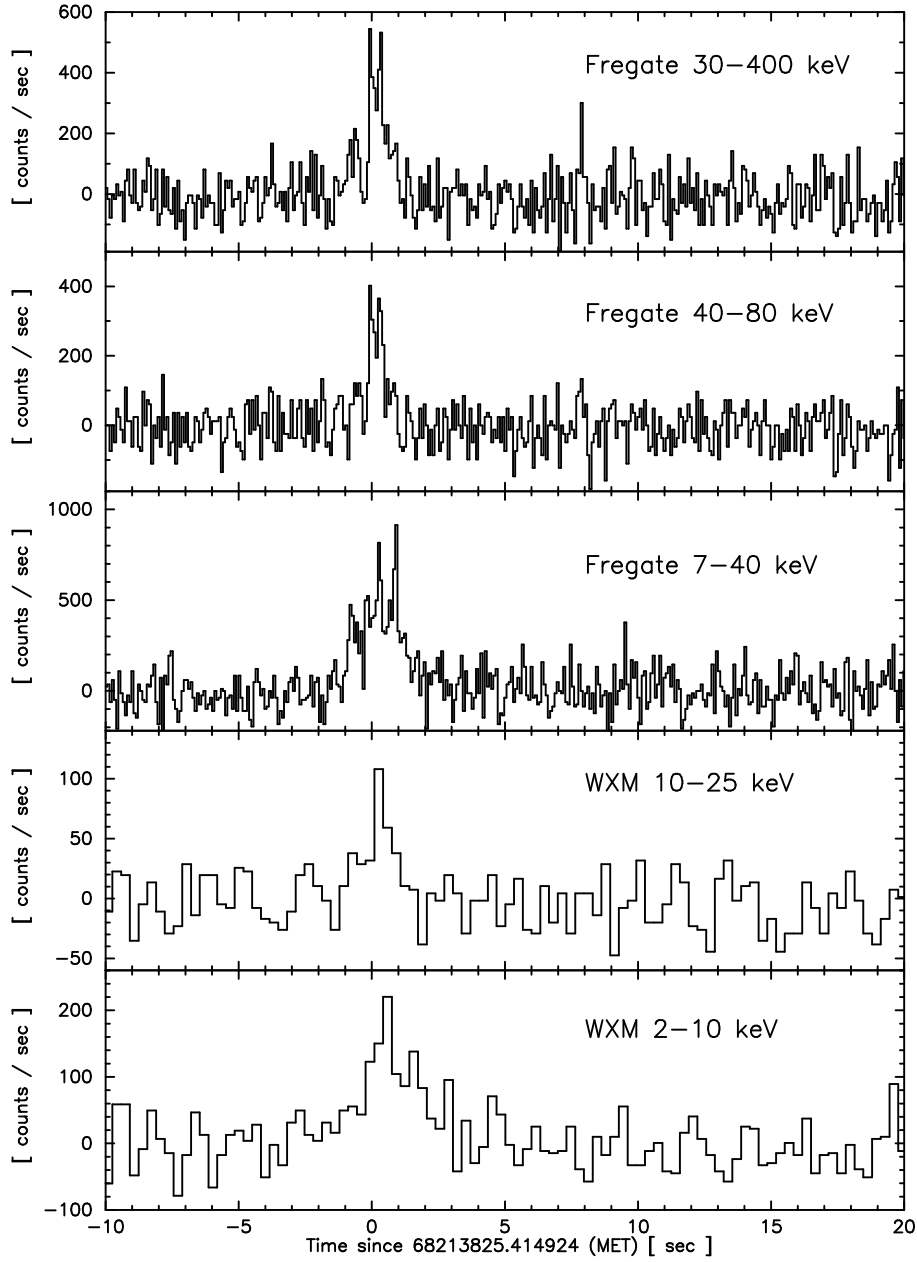


Fig. 2.— Time history of GRB 010326B in various energy bands. The average background level before the burst has been subtracted. The Fregate counts are binned at 82 msec and the WXM counts are binned at 328 msec.

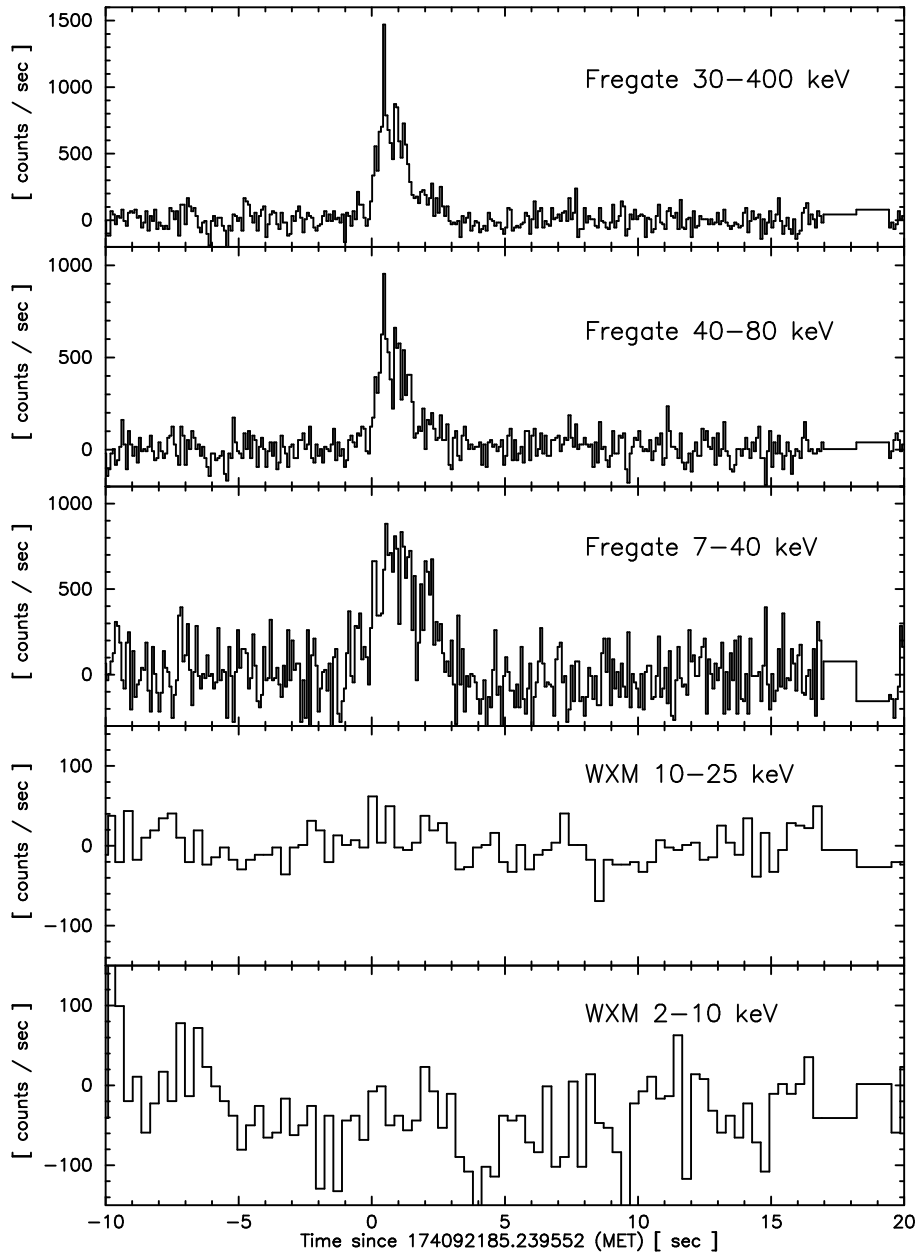


Fig. 3.— Time history of GRB 040802 in various energy bands. The average background level before the burst has been subtracted. The Fregate counts are binned at 82 msec and the WXM counts are binned at 328 msec.



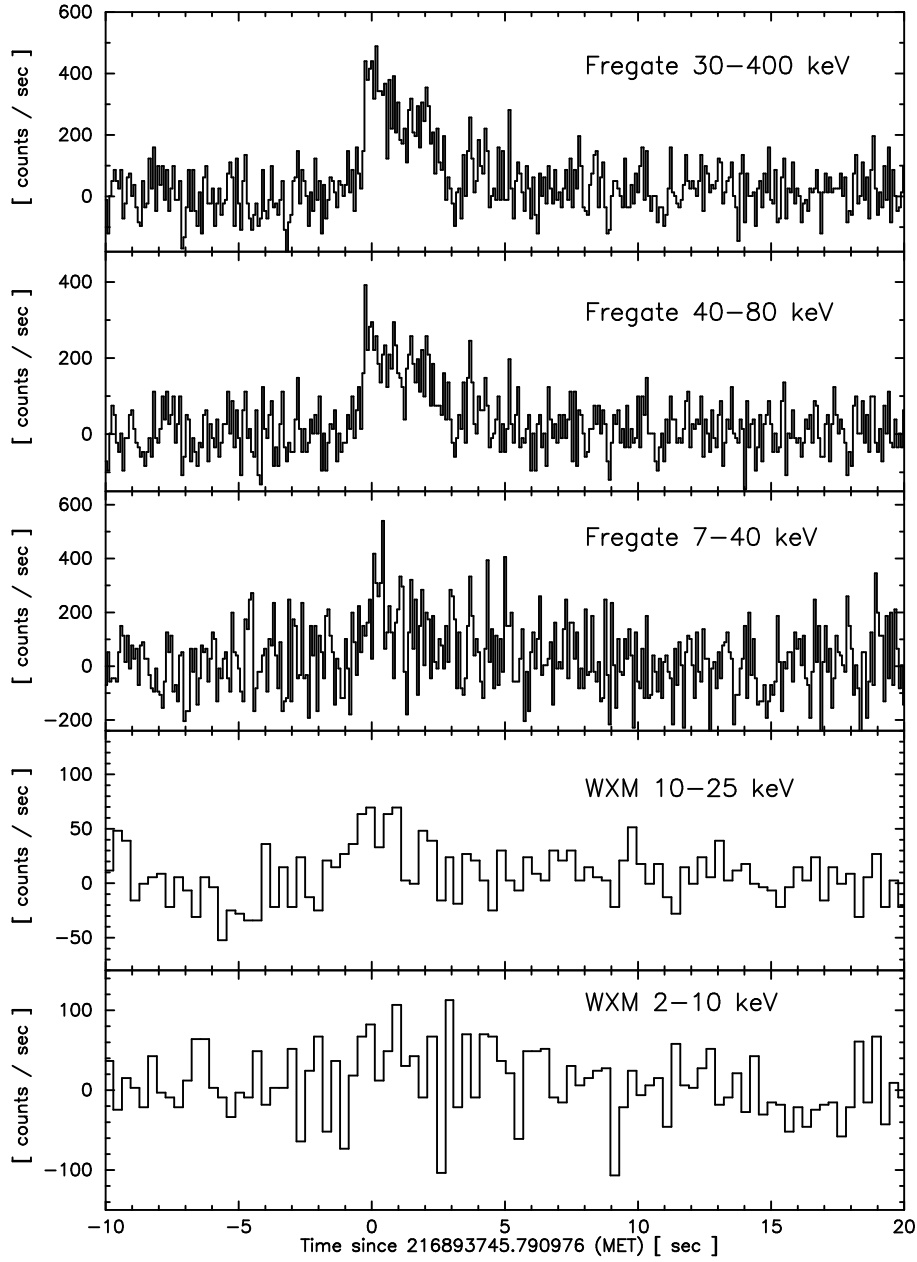


Fig. 4.— Time history of GRB 051211 in various energy bands. The average background level before the burst has been subtracted. The Fregate counts are binned at 82 msec and the WXM counts are binned at 328 msec.

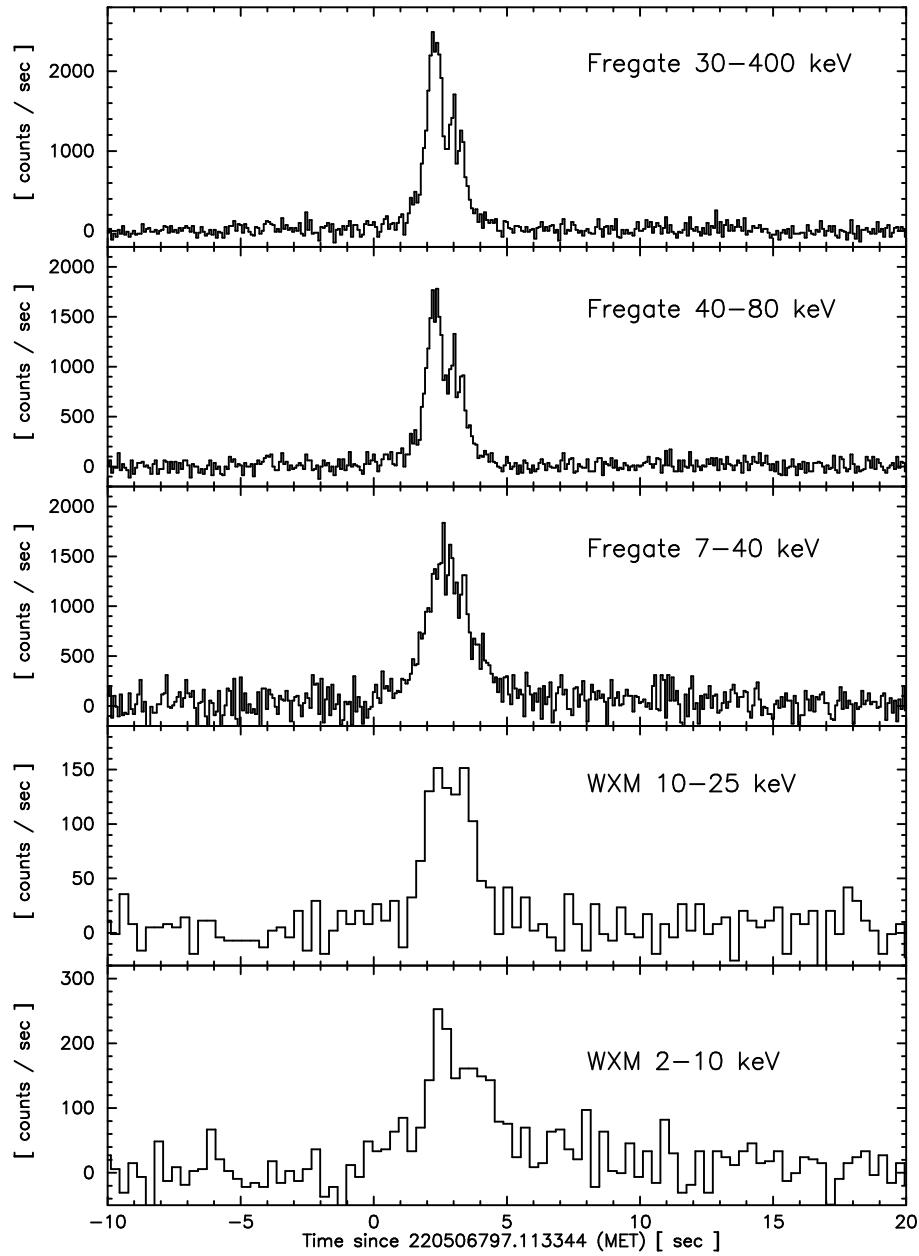


Fig. 5.— Time history of GRB 060121 in various energy bands. The average background level before the burst has been subtracted. The Fregate counts are binned at 82 msec and the WXM counts are binned at 328 msec.

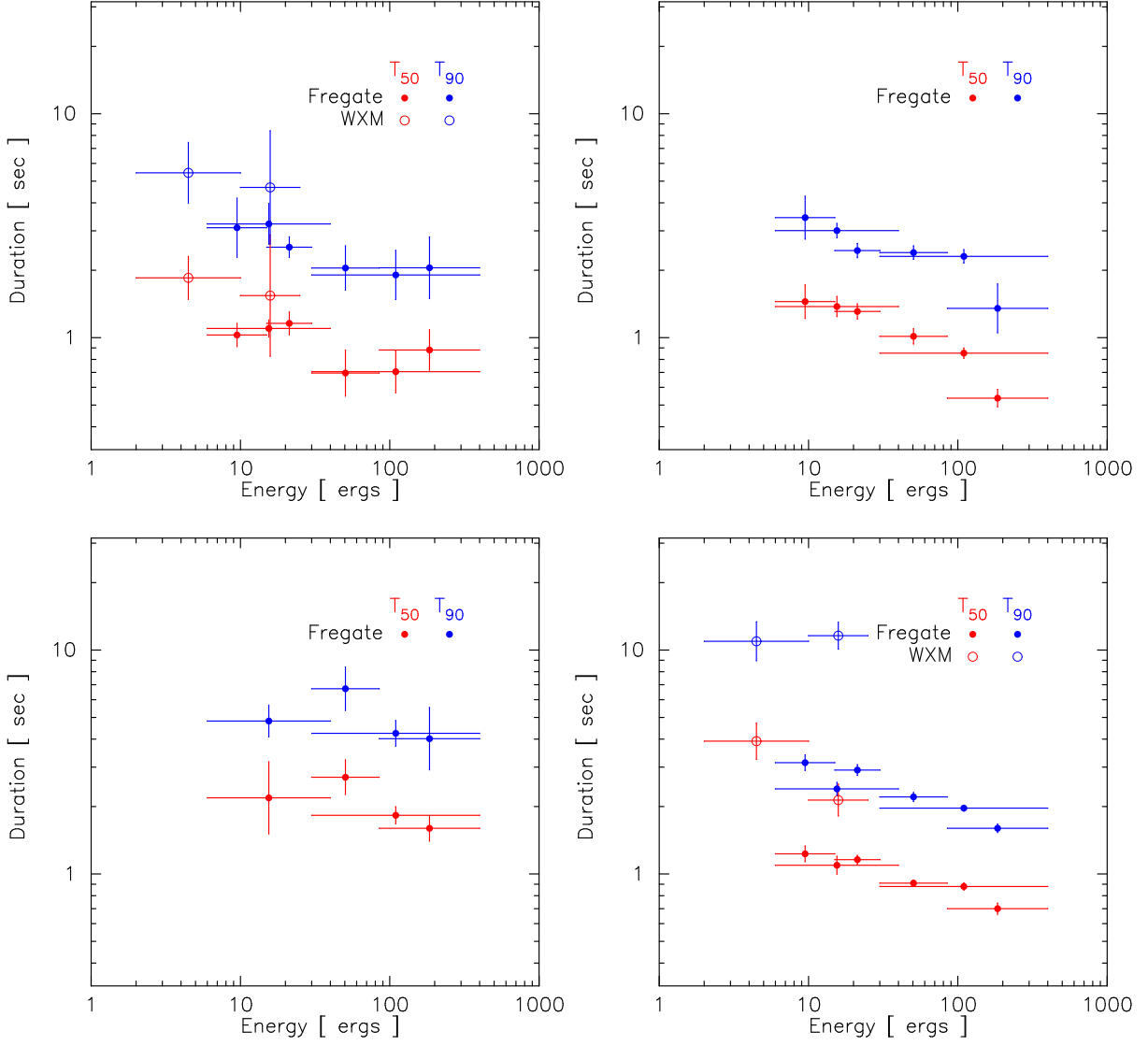


Fig. 6.— Duration measures as a function of energy for GRBs 010326B (upper left), 040802 (upper right), 051211 (lower left) and 060121 (lower right). Fregate durations are provided for the 6–15 keV, 15–30 keV, 30–85 keV, 85–300 keV, 6–40 keV, and 30–400 keV bands (when available); WXM durations are provided for the 2–10 keV and 10–15 keV bands (when available). See Table 2 for the data.

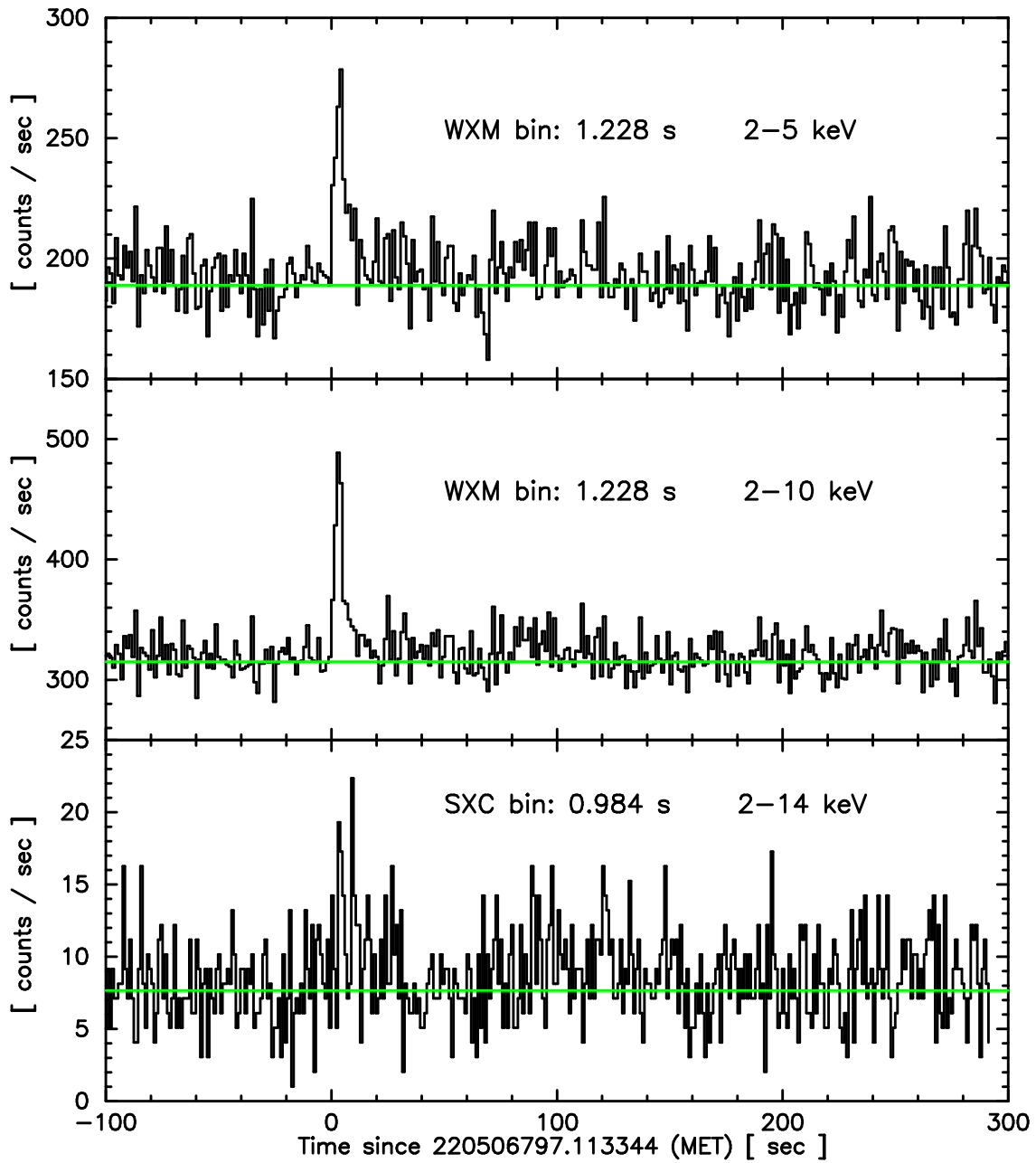


Fig. 7.— WXM and SXC lightcurves for GRB 060121 showing the softer emission following the short, hard spike. The WXM data is binned in 1.228 sec bins for the 2-5 keV band (top) and the 2-10 keV band (middle). The SXC data is binned in 0.984 sec bins with an approximate energy range of 2-14 keV. The green line shows the average background level from before the burst.

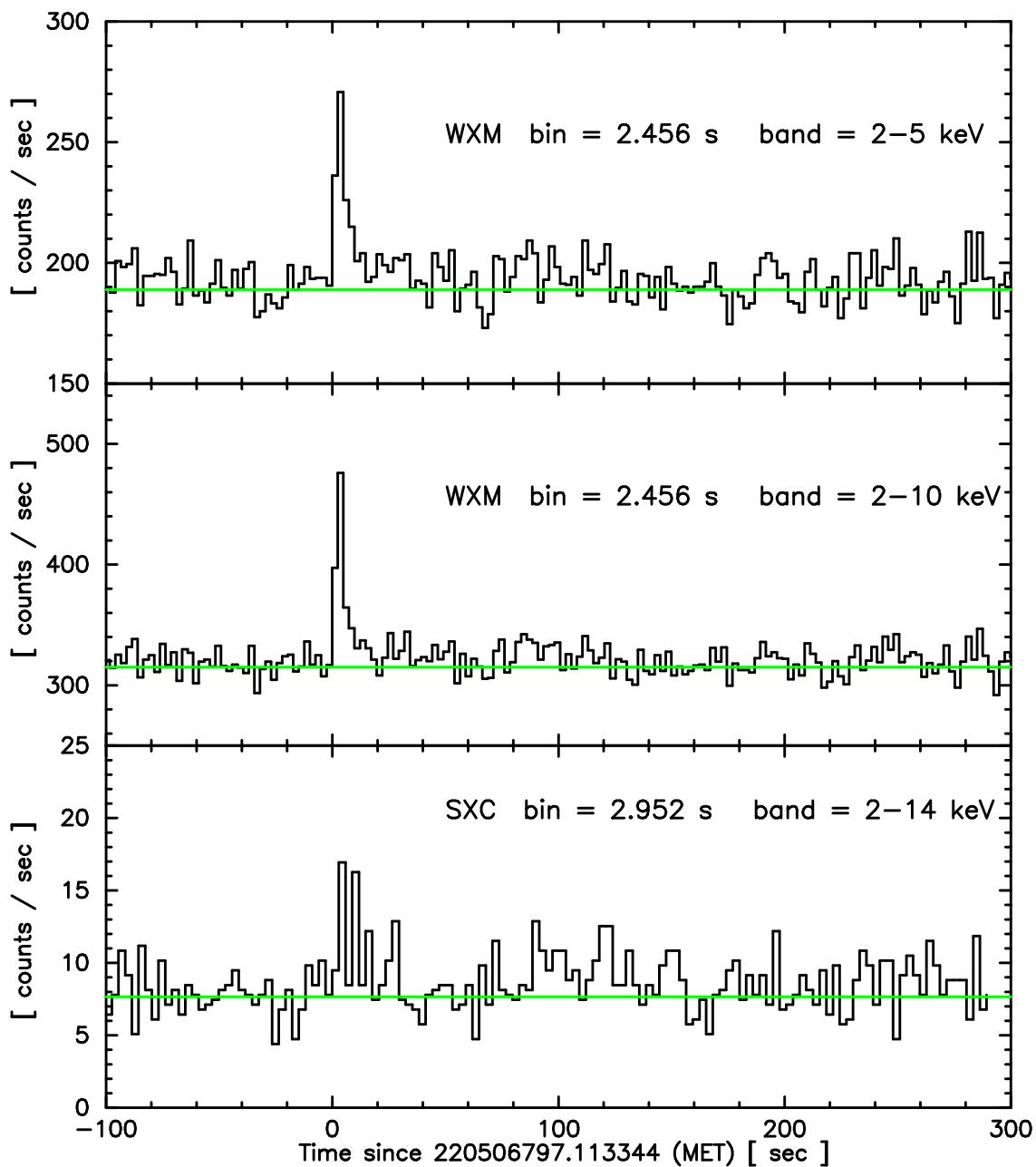


Fig. 8.— WXM and SXC lightcurves for GRB 060121 showing the softer emission following the short, hard spike. The WXM data is binned in 2.456 sec bins for the 2-5 keV band (top) and the 2-10 keV band (middle). The SXC data is binned in 2.952 sec bins with an approximate energy range of 2-14 keV. The green line shows the average background level from before the burst.

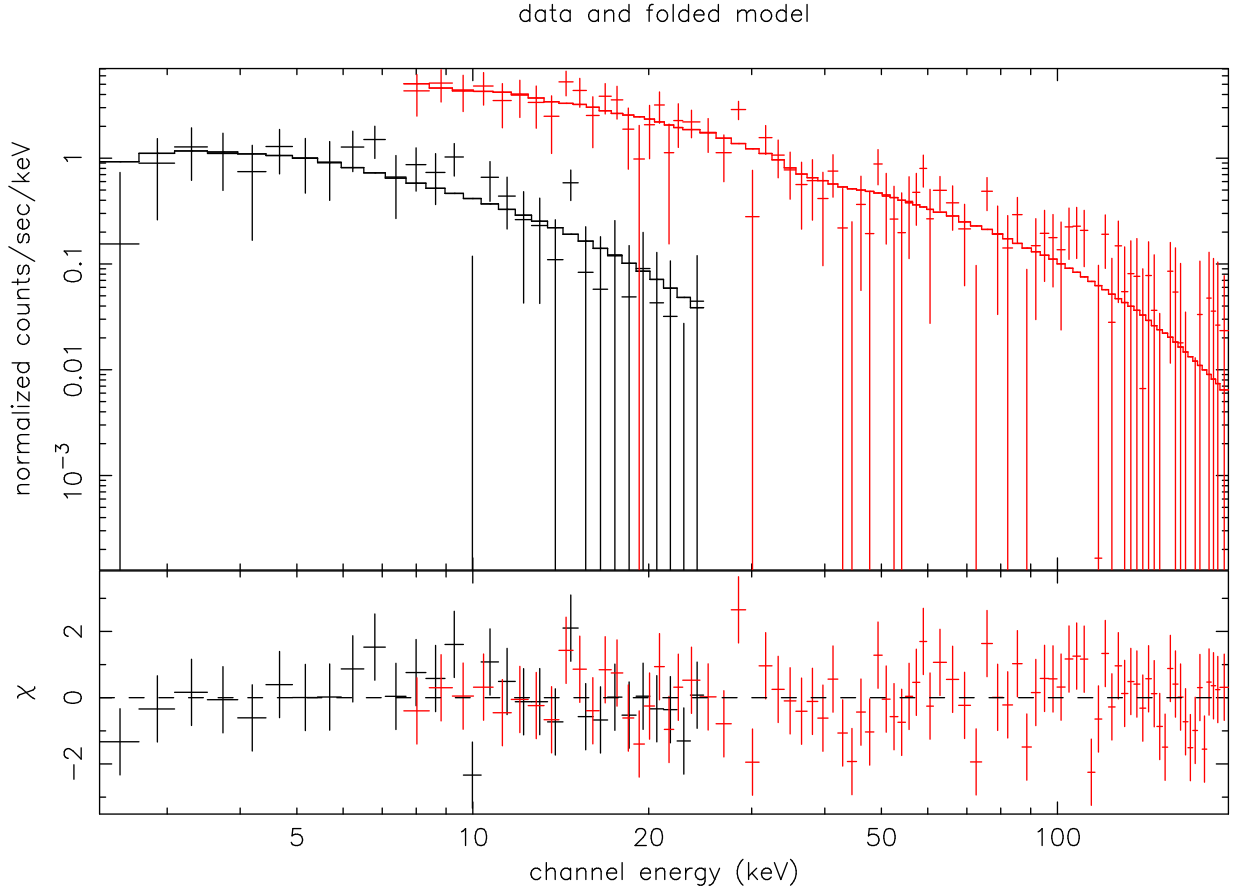


Fig. 9.— Comparison of the observed and predicted spectrum of GRB 010326B in count space. The upper panel compares the counts in the WXM energy loss channels (black points) and the Fregate energy loss channels (red points) and those predicted by the best-fit cutoff power-law spectral model ( $\alpha = -1.08^{+0.25}_{-0.22}$  and  $E_{\text{peak}}^{\text{obs}} = 51.8^{+18.6}_{-11.3}$  keV); the lower panel shows the residuals to the fit.

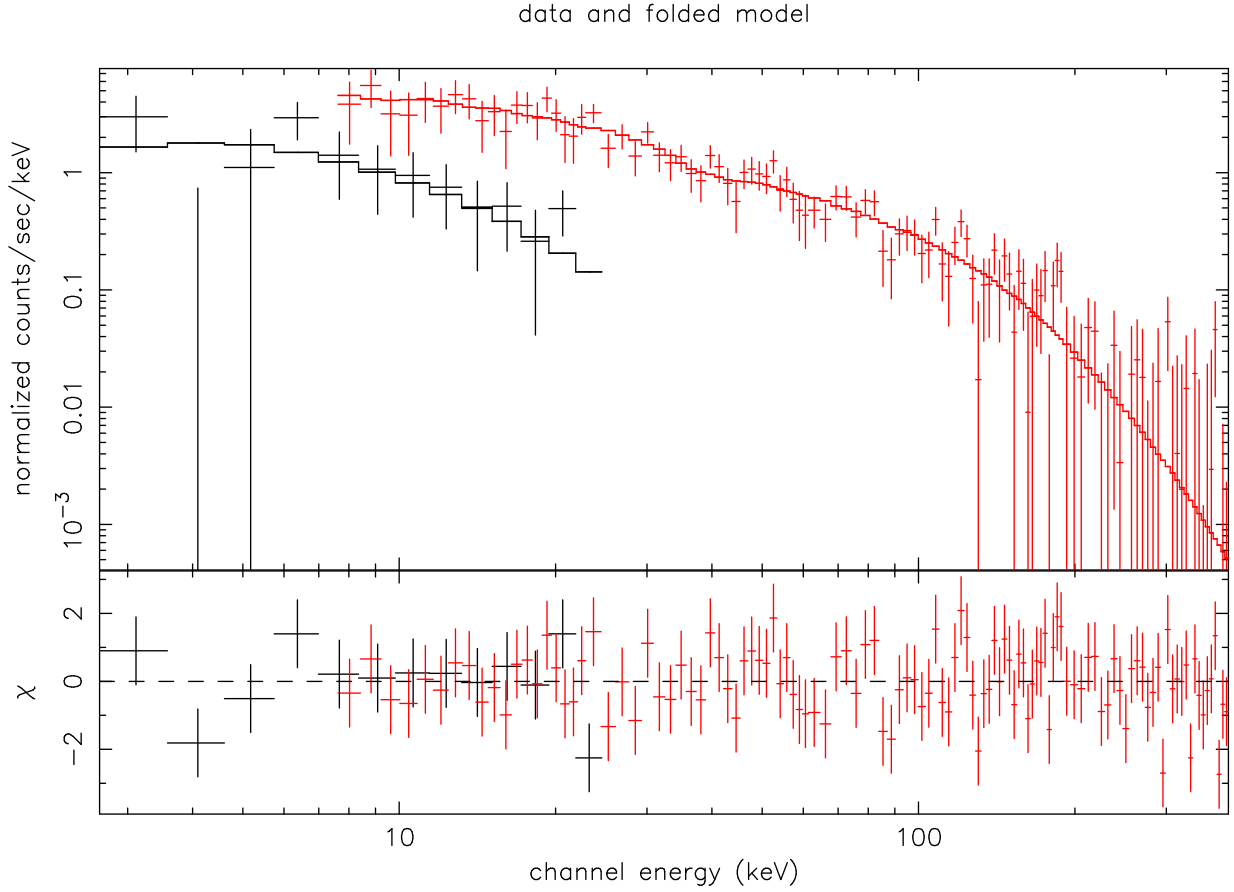


Fig. 10.— Comparison of the observed and predicted spectrum of GRB 040802 in count space. The upper panel compares the counts in the WXM energy loss channels (black points) and the Fregate energy loss channels (red points) and those predicted by the best-fit cutoff power-law spectral model ( $\alpha = -0.85_{-0.20}^{+0.23}$  and  $E_{\text{peak}}^{\text{obs}} = 92.2_{-13}^{+18.8}$  keV); the lower panel shows the residuals to the fit.

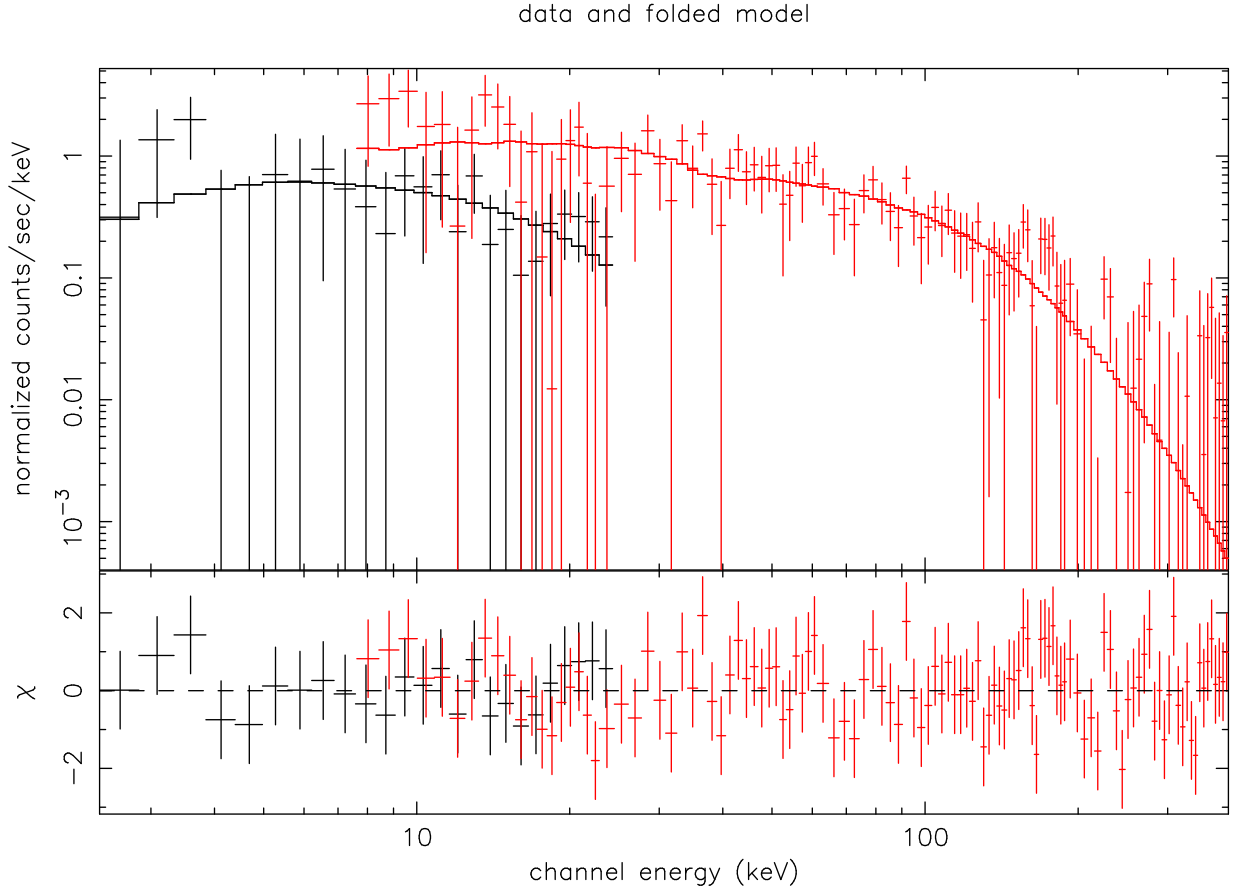


Fig. 11.— Comparison of the observed and predicted spectrum of GRB 051211 in count space. The upper panel compares the counts in the WXM energy loss channels (black points) and the Fregate energy loss channels (red points) and those predicted by the best-fit cutoff power-law spectral model ( $\alpha = -0.07^{+0.50}_{-0.41}$  and  $E_{\text{peak}}^{\text{obs}} = 121^{+33.0}_{-20.3}$  keV); the lower panel shows the residuals to the fit.



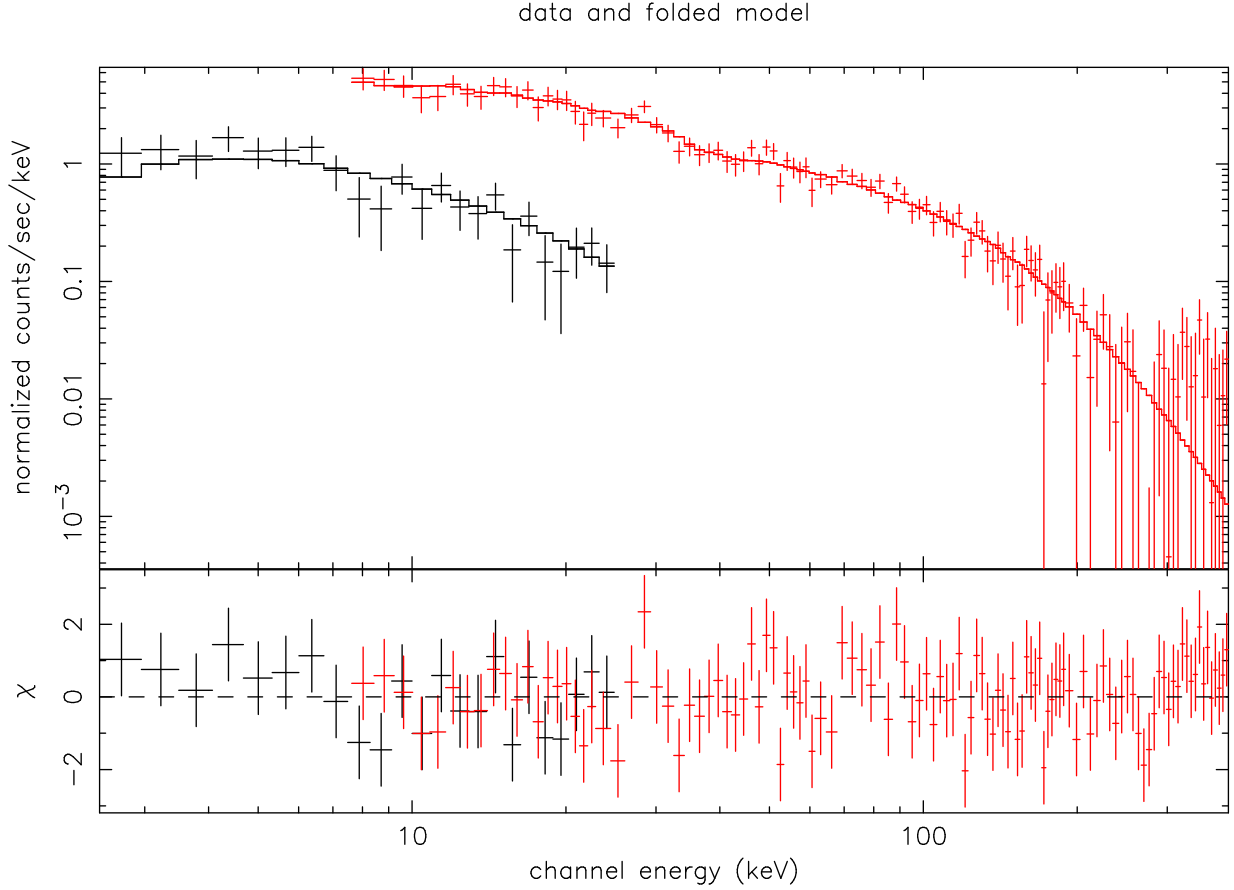


Fig. 12.— Comparison of the burst-averaged observed and predicted spectrum of GRB 060121 in count space. The upper panel compares the counts in the WXM energy loss channels (black points) and the Fregate energy loss channels (red points) and those predicted by the best-fit cutoff power-law spectral model ( $\alpha = -0.79^{+0.12}_{-0.11}$  and  $E_{\text{peak}}^{\text{obs}} = 114^{+14.2}_{-10.9}$  keV); the lower panel shows the residuals to the fit.

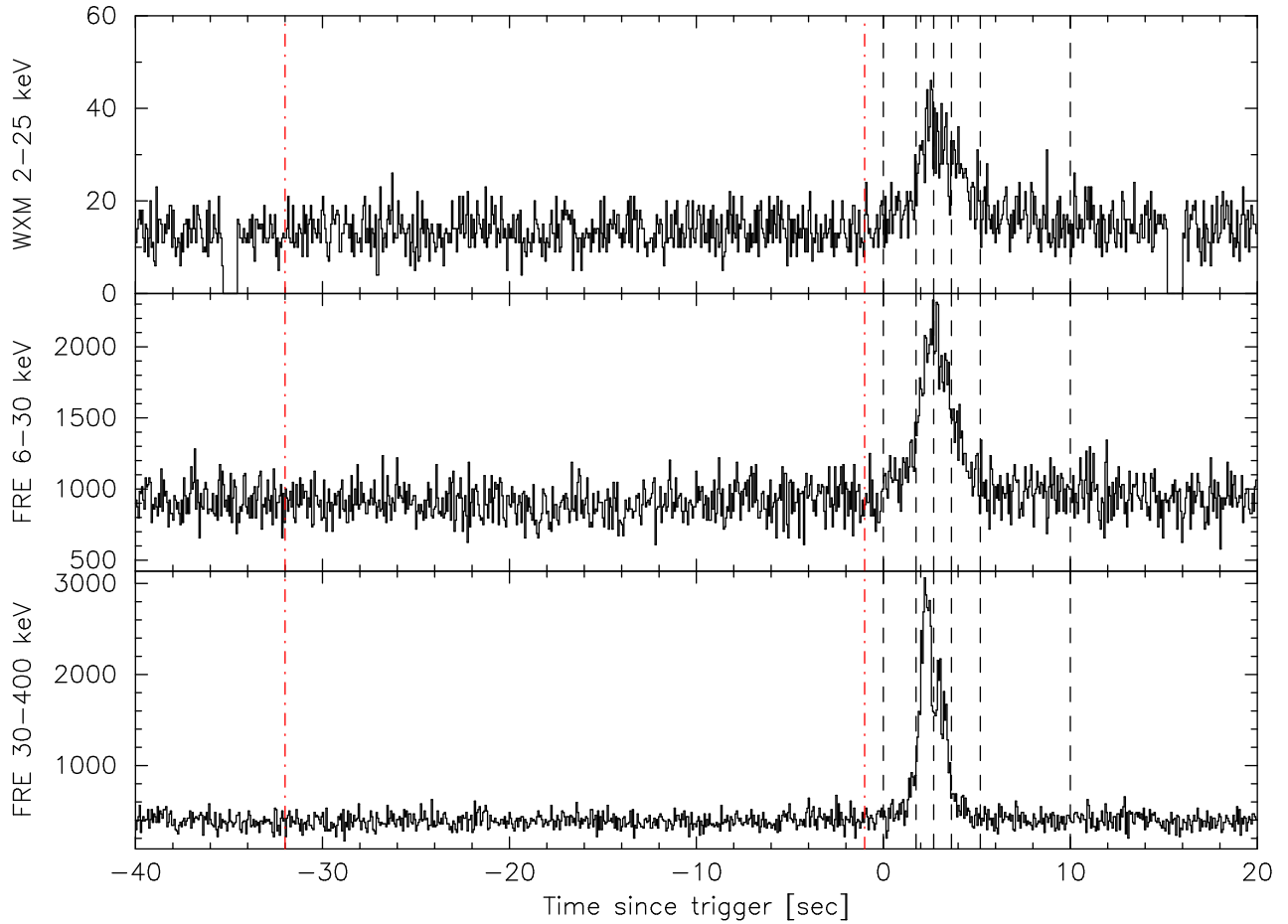


Fig. 13.— WXM and Fregate lightcurves of GRB 060121 showing the background (red dot-dash lines) and 5 foreground regions (black dashed lines starting at  $t=0$ ) used for the time-resolved spectral analysis.

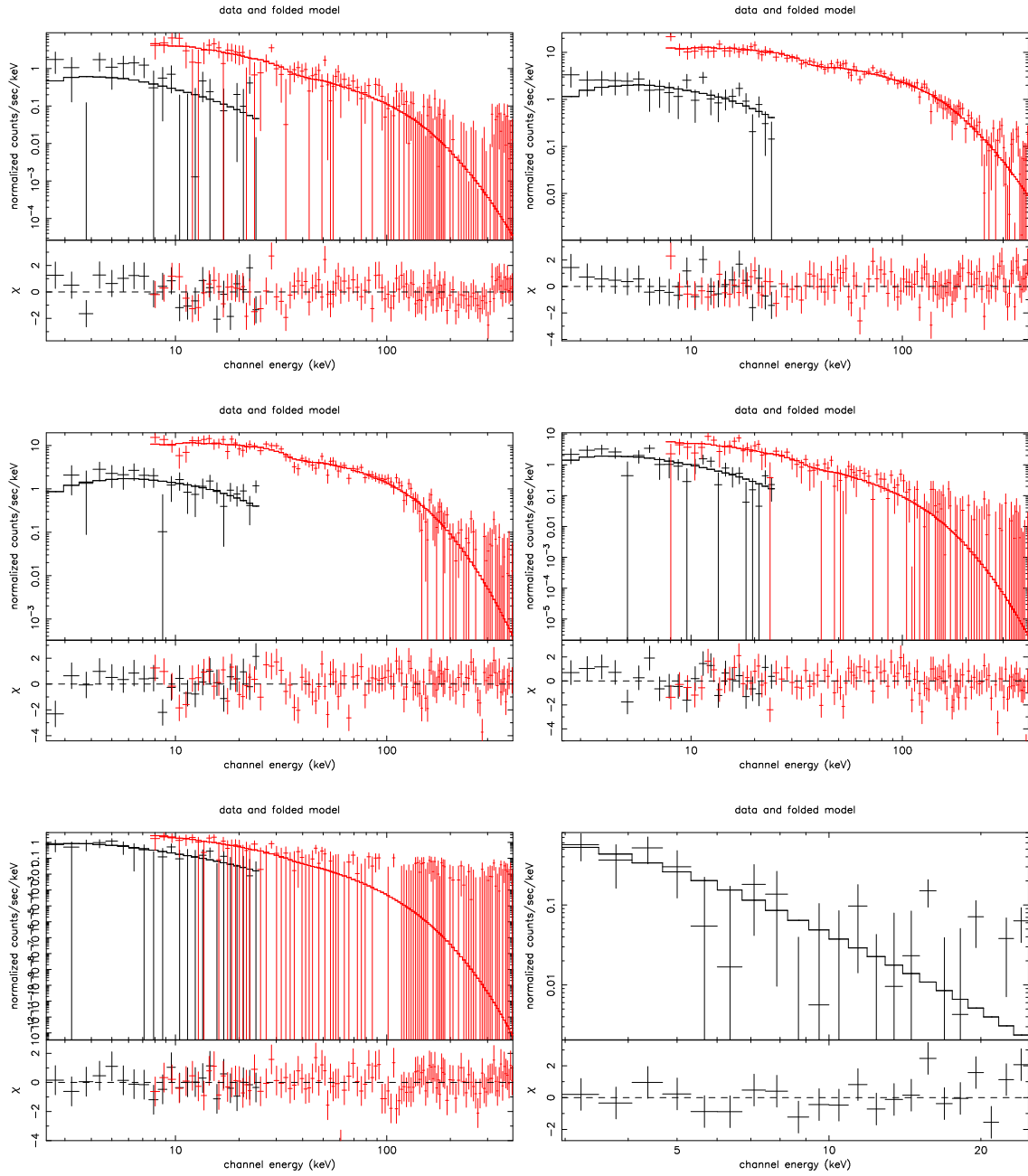


Fig. 14.— Counts spectra for five time regions showing the spectral evolution of GRB 060121: 0-1.75 sec (upper left), 1.75-2.7 sec (upper right), 2.7-3.64 sec (middle left), 3.64-5.186 sec (middle right), 5.186-10 sec (bottom left) and the soft bump from 71.2-121.6 sec (bottom right).

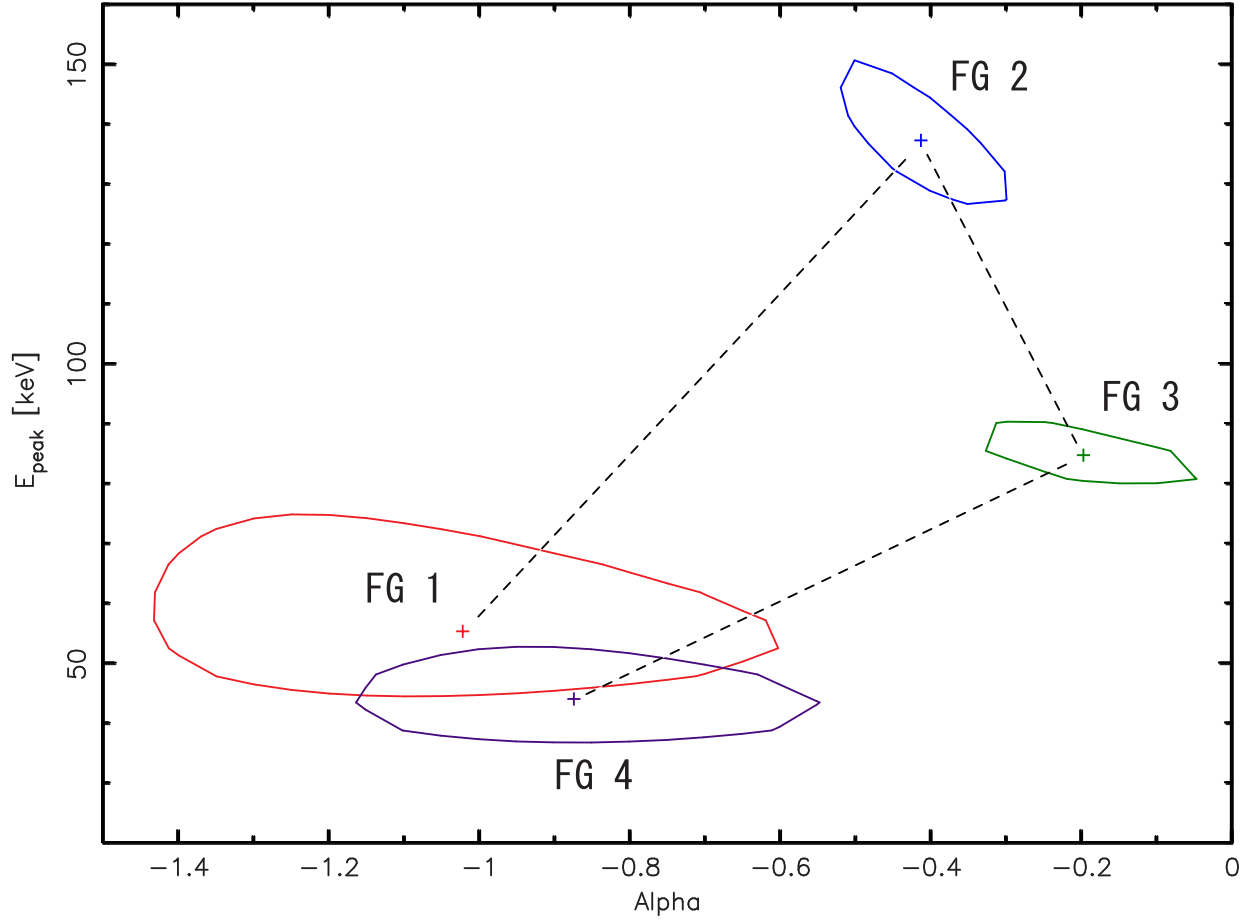


Fig. 15.— 68% confidence level contours in the  $[\alpha, E_{\text{peak}}^{\text{obs}}]$ -plane showing the spectral evolution of GRB 060121 through four time intervals. Clockwise from the left, the regions correspond to time regions 1 (red, 0-1.75 sec), 2 (blue, 1.75-2.7 sec), 3 (green, 2.7-3.64 sec) and 4 (purple, 3.64-5.186 sec).

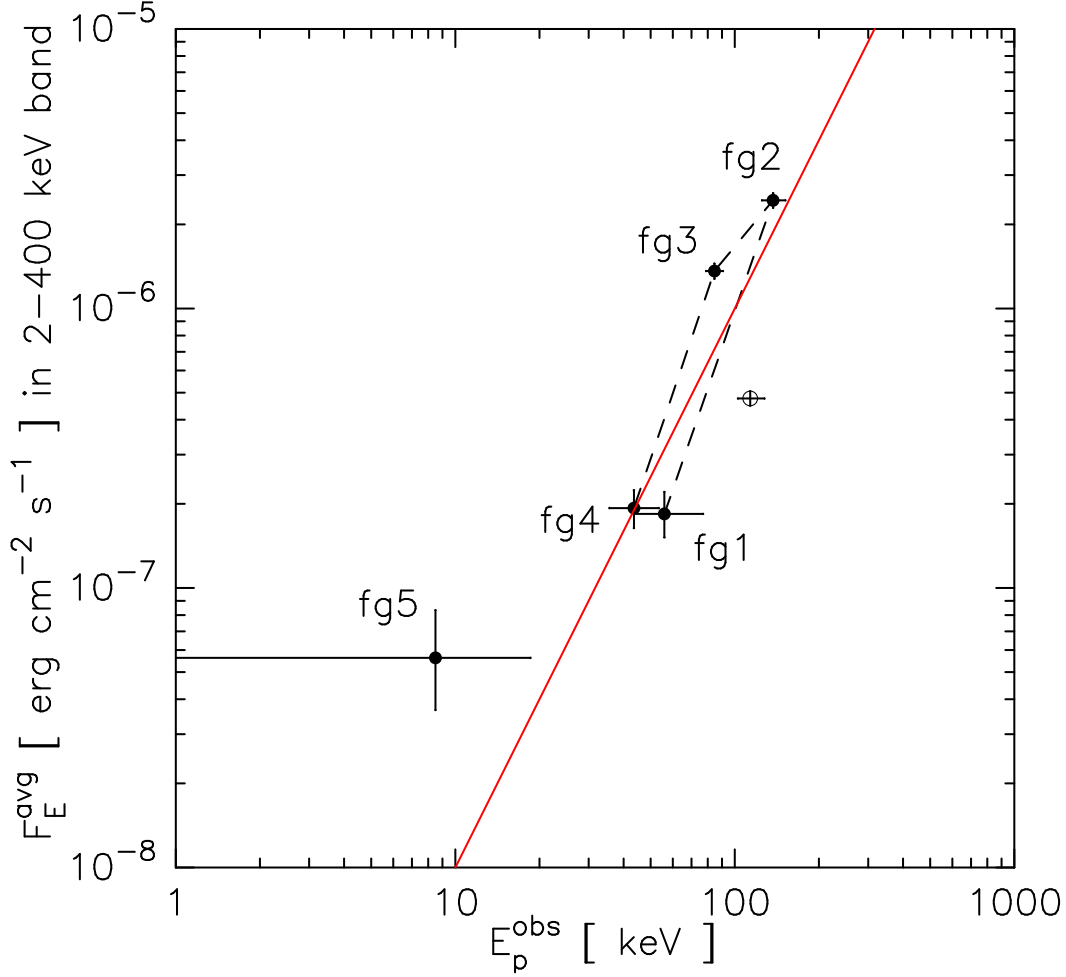


Fig. 16.— Plot of the GRB 060121 time regions in the  $[E_{\text{peak}}^{\text{obs}}, F_E^{\text{avg}}(2-400)]$ -plane. The four solid black points connected by the dashed line correspond, counter-clockwise to the time regions 1 (0-1.75 sec), 2 (1.75-2.7 sec), 3 (2.7-3.64 sec) and 4 (3.64-5.186 sec). The unconnected point in the lower left corresponds to the time region 5 (5.186-10.0 sec). The open circle represents the burst-averaged quantities. The solid red line represents a slope of 2.

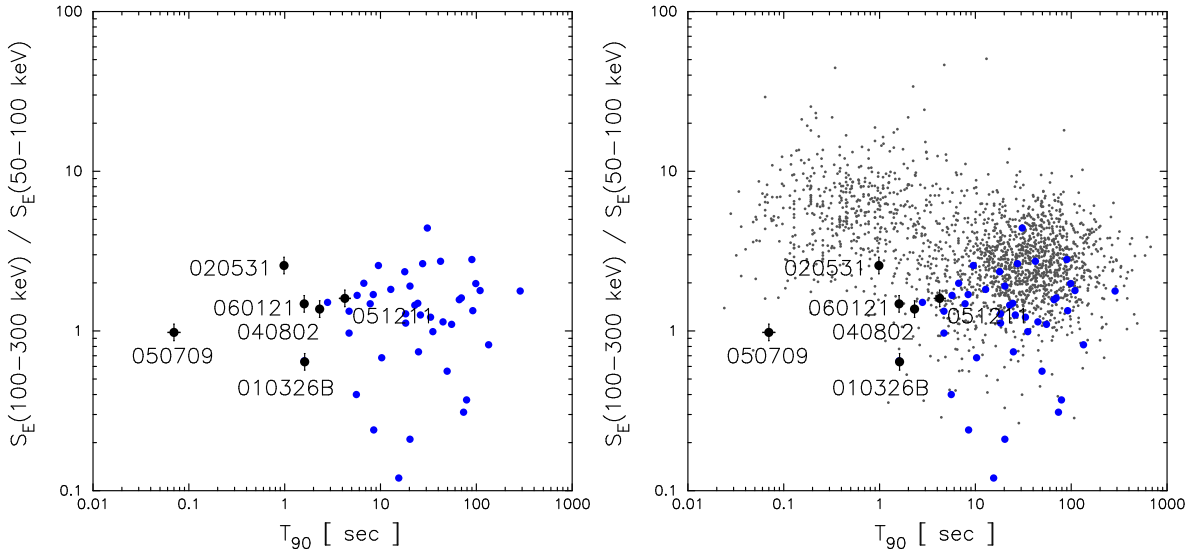


Fig. 17.— Left panel: Comparison of the locations in the  $[T_{90}, S(100 - 300)/S(50 - 100)]$ -plane of six HETE-2 short bursts (GRBs 010326B, 020531, 040802, 050709, 051211 and 060121) and 42 HETE-2 long GRBs (blue points). Right panel: Comparison of the locations in the  $[T_{90}, S(100 - 300)/S(50 - 100)]$ -plane of six HETE-2 short GRBs and 42 HETE-2 long GRBs (blue points) and 1973 BATSE bursts (gray points) with six HETE-2 short GRBs. The extension of the HETE-2 long bursts to lower hardness ratio than the BATSE sample is due to the ability of HETE-2 to trigger on soft X-Ray-Flashes (Sakamoto et al. 2006).

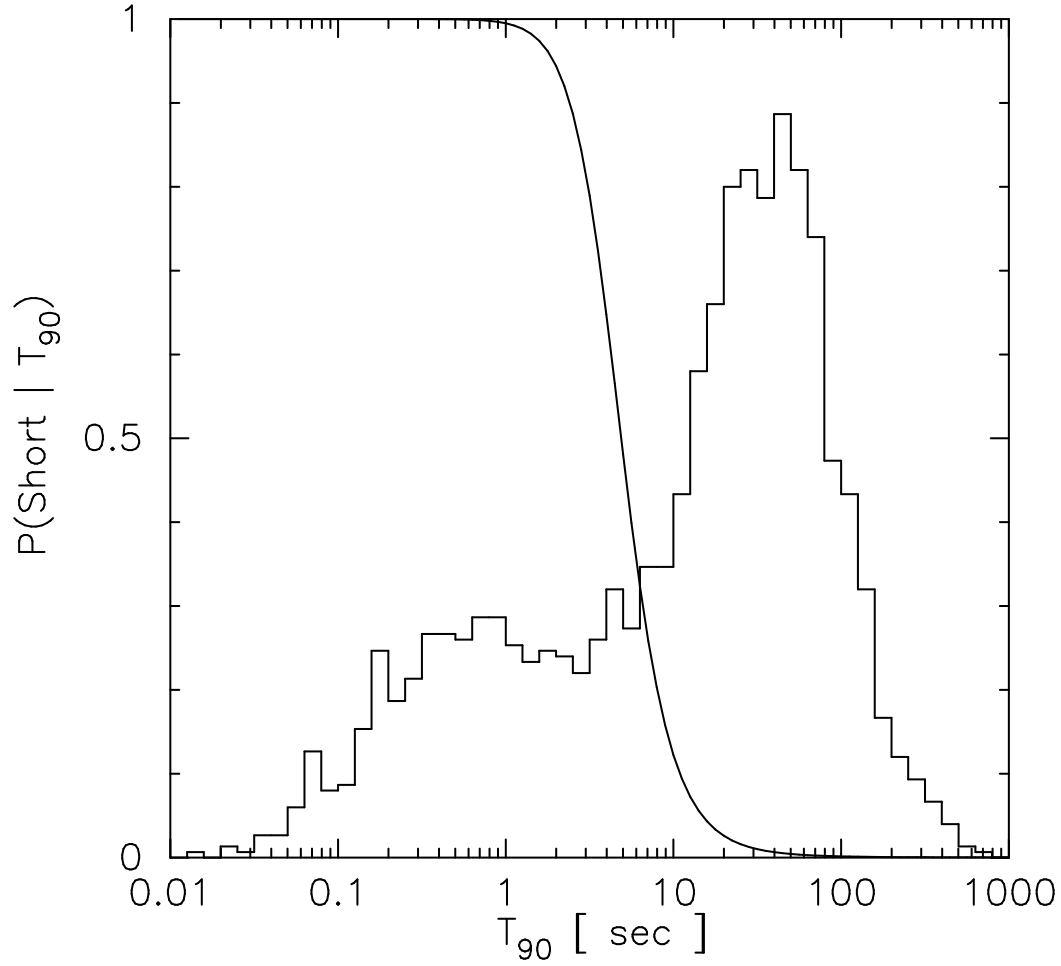


Fig. 18.— Probability that a burst belongs to the short population as a function of  $T_{90}$ , plotted on top of the BATSE duration distribution.

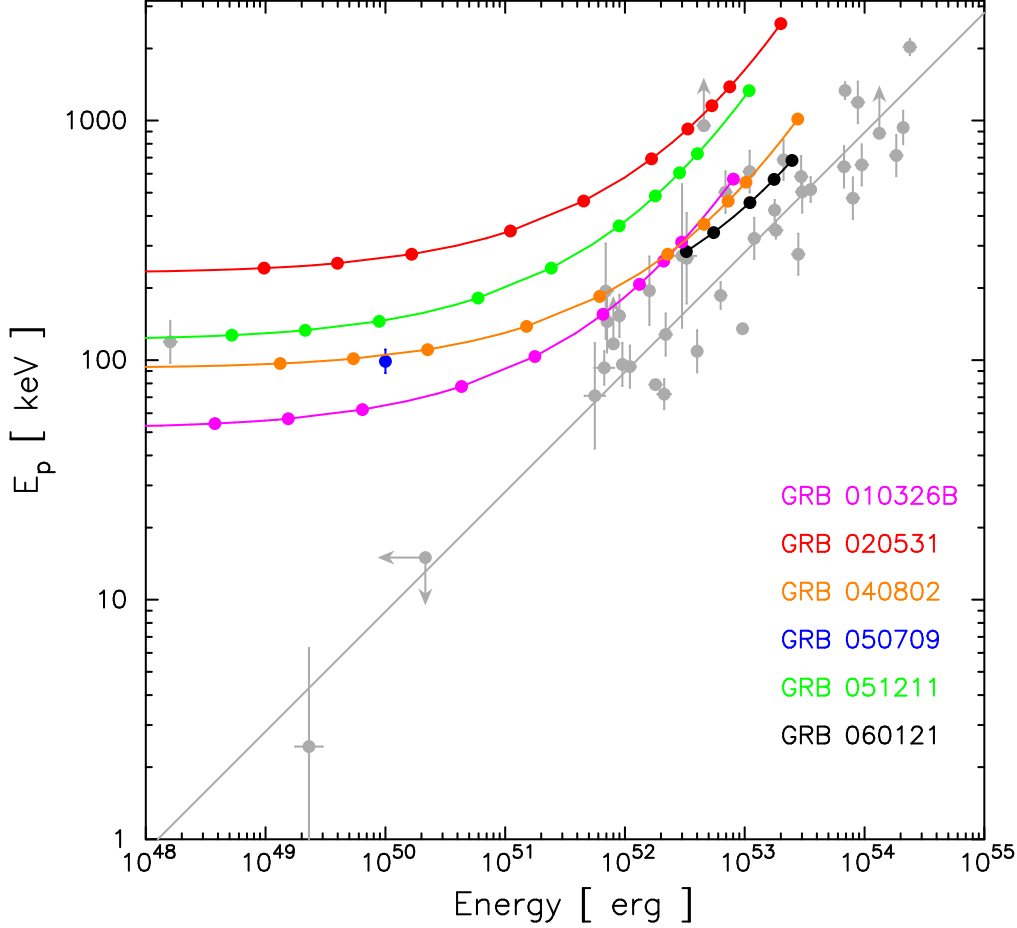


Fig. 19.— Comparison of the six HETE-2 short bursts with known  $E_{\text{peak}}$  values, with the observed  $E_{\text{peak}} \propto E_{\text{iso}}^{1/2}$  relation for long GRBs (gray points). Shown are GRBs 050709 (blue,  $z=0.16$ ), 010326B (magenta trajectory), 020531 (red), 040802 (orange), 051211 (green) and 060121 (black). For burst without known redshift, the points along the trajectory correspond, from left to right, with burst redshifts  $z=0.05, 0.1, 0.2, 0.5, 1, 2, 3, 4, 5$  and  $10$ . GRB 060121 is constrained to lie between  $z=1.5$  and  $4.6$ , so we plot here a trajectory with points at  $z=1.5, 2, 3, 4$  and  $5$ .